

# STARSHADE TECHNOLOGY STATUS: OPTICS

Stuart Shaklan  
Jet Propulsion Laboratory, California Institute of Technology

Starshade S5 Closeout Review  
April 14, 2025

# STATE OF TECHNOLOGY: STARSHADE OPTICS

The goal of this presentation is to describe the main results of S5 Optics work covering Milestones 1-4.

- **Optical Diffraction (M1):**
  - Demonstrated  $< 1e-10$  contrast, broadband, diffraction and polarization models validation at flight Fresnel Number
- **Sensitivity to Shape Perturbations (M2):**
  - Measured sensitivity of starlight leakage (contrast) to petal shape and position.
  - Measured model uncertainty factor incorporated into starshade shape error budgets.
- **Formation Flying (M4):**
  - Optical demo of sensing signal, model of alignment and telescope pointing, model of flight control loop
  - Hardware-in-the-loop closed loop demo
- **Solar Scatter (M3):**
  - Measured scatter of coated and uncoated edges,
  - Experimental contamination study leading to particulate contamination requirements
  - Detailed modeling of surfaces and interfaces leading to starshade planarity requirements
- **Micrometeoroids (M3+):**
  - Detailed study of expected level of starlight leakage and solar scatter from micrometeoroid damage
- **Imaging Simulation:**
  - Developed Starshade Imaging Simulation Toolkit for Exoplanet Reconnaissance (SISTER)

# Milestones 1A and 1B: Starlight Suppression + Model Validation

**Milestone 1A:** Small-scale starshade mask in the Princeton Testbed demonstrates  $1 \times 10^{-10}$  instrument contrast at the inner working angle in *narrow* band visible light and Fresnel number  $\leq 15$ .

**Milestone 1B:** Small-scale starshade mask in the Princeton Testbed demonstrates  $1 \times 10^{-10}$  instrument contrast at the inner working angle at *multiple wavelengths* spanning  $\geq 10\%$  bandpass and Fresnel number  $\leq 15$  at the longest wavelength.

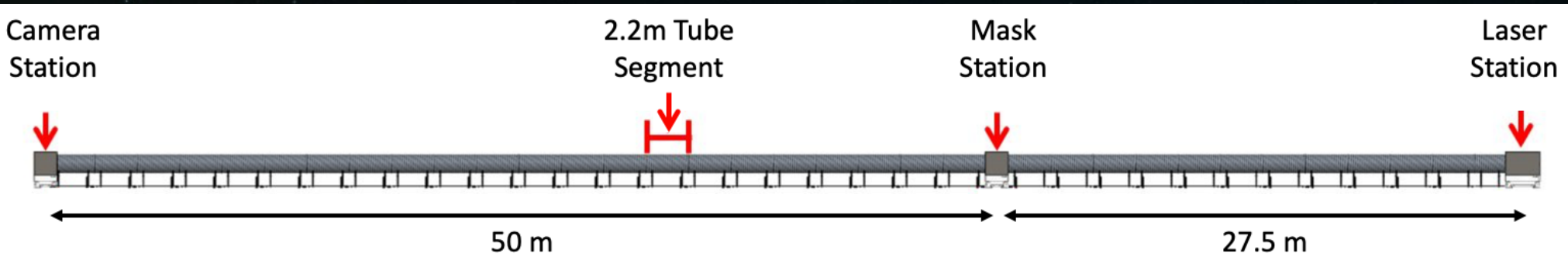
# PRINCETON STARSHADE TESTBED



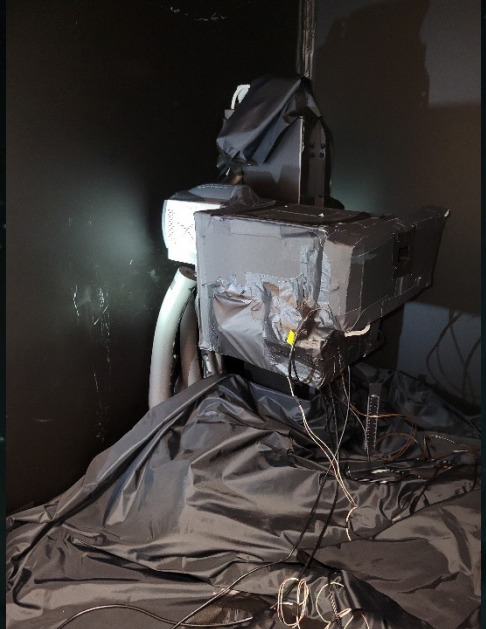
5-cm diameter Starshade  
etched in silicon

**A. Harness et al references:** M1a,b reports, JATIS, SPIE  
Shaklan et al M2 report

- 80 m long tube in basement of Frick building on Princeton campus
- Not evacuated (1 atm)
- Point source, starshade mask, simple camera.
- Remotely operated
- Settling time for 1e-10 contrast was about 3 days.
- Operational 2017-2022.



# TESTBED IMAGES



Camera



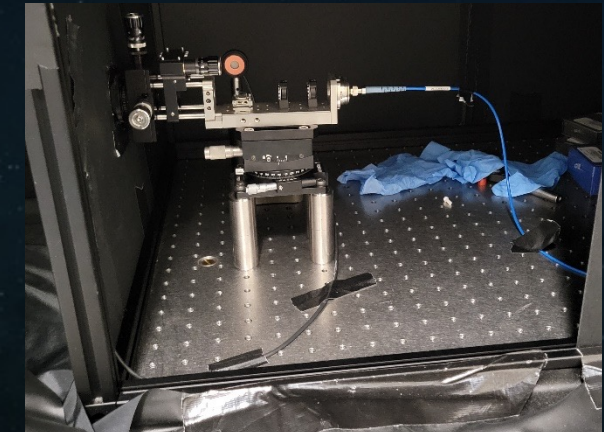
Mask Station



Mask



In the tube

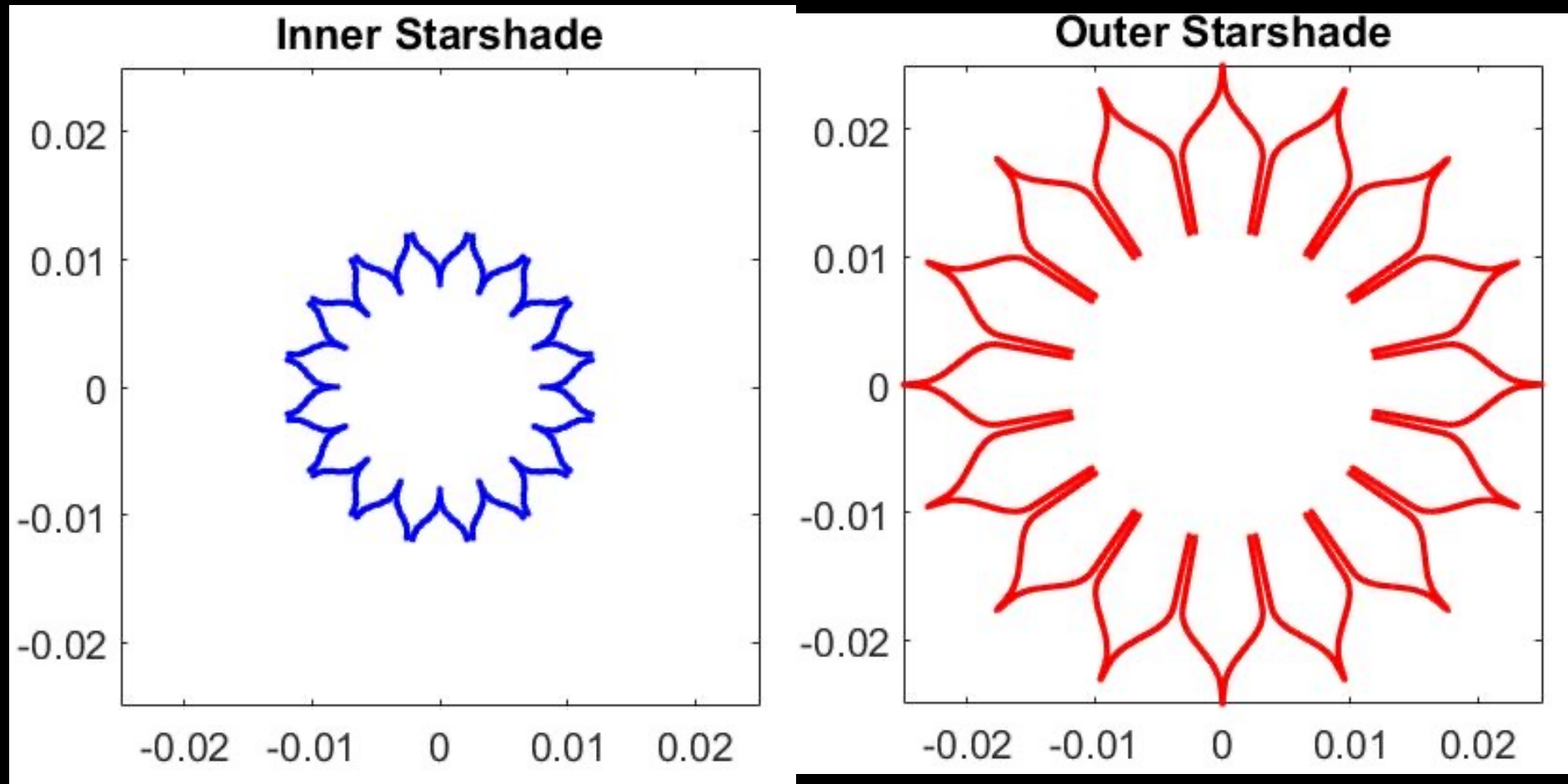


Laser point source

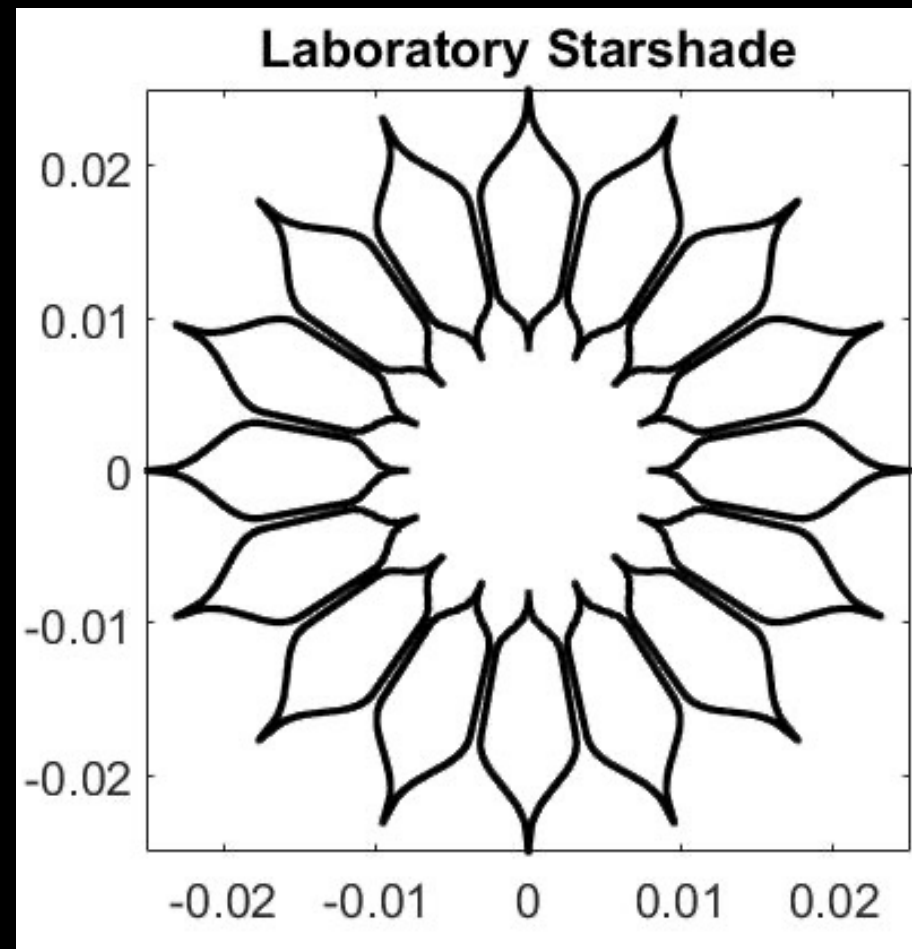
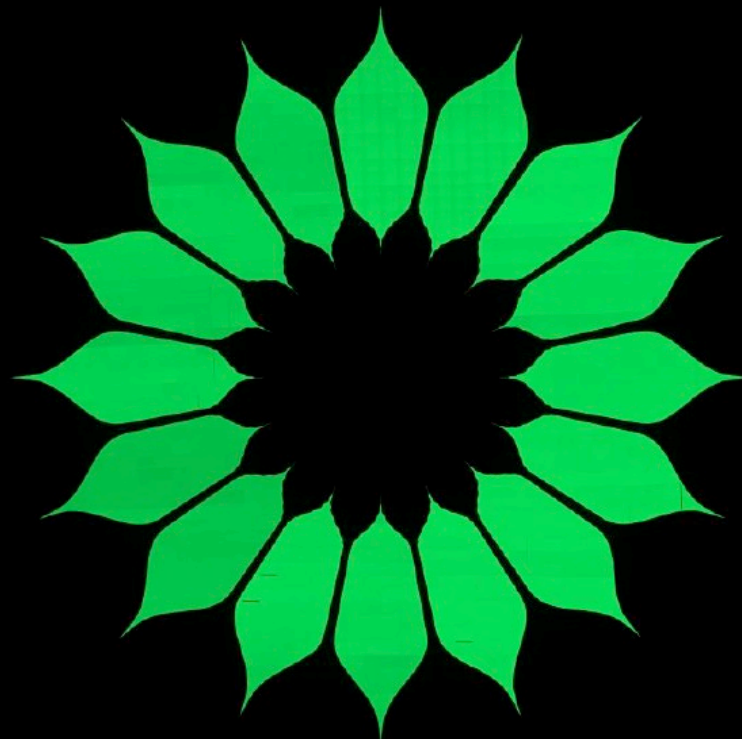


Lasers, 641, 660,  
699, 725 nm

# LABORATORY STARSHADE DESIGN



# LABORATORY STARSHADE DESIGN



# HOW IS A MINIATURE STARSHADE SIMILAR TO FLIGHT STARSHADE?

Physics is identical for consistent Fresnel number

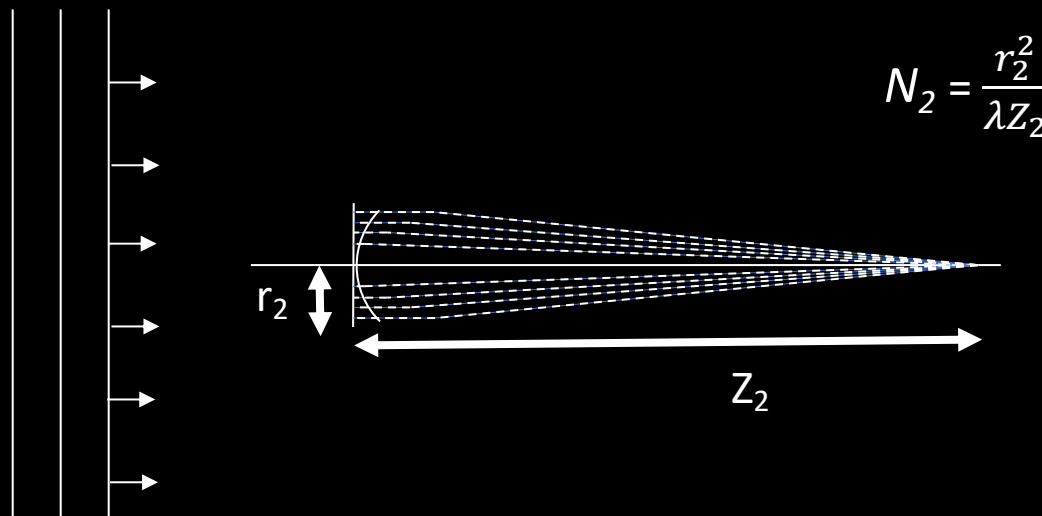
- Under scalar diffraction + Fresnel approximations

$$U(p) \propto \frac{-i}{\lambda z} \iint e^{\frac{i\pi r^2}{\lambda z}} r dr d\theta$$

Fresnel Number

$$N = \frac{r^2}{\lambda z}$$
$$\propto \frac{-i}{2} \iint e^{i\pi N} dN d\theta$$

- Same integrand
- Same integration limits relative to integrand
- Small mask has a much larger 3<sup>rd</sup> order term relative to the Fresnel approximation. Larger starshade is a better Fresnel approximation.



$$N_2 = \frac{r_2^2}{\lambda z_2}$$

$$r_2 = 30 \text{ m}$$

$$Z_2 = 95,200 \text{ km}$$

$$\lambda = 781 \text{ nm}$$

$$N_2 = 12.1$$

$$\text{Tel. Res} = 2.4 \lambda/D$$

$$3^{\text{rd}} \text{ order}/2^{\text{nd}} \text{ order} = 2.5 \times 10^{-14}$$

$N_1 = N_2$ : Maintaining Fresnel Number preserves the math/physics. Higher order terms are less important at large scale.

# HOW IS A MINIATURE STARSHADE SIMILAR TO AN ORBITING STARSHADE?

Physics is identical for consistent Fresnel number

- Under scalar diffraction + Fresnel approximations

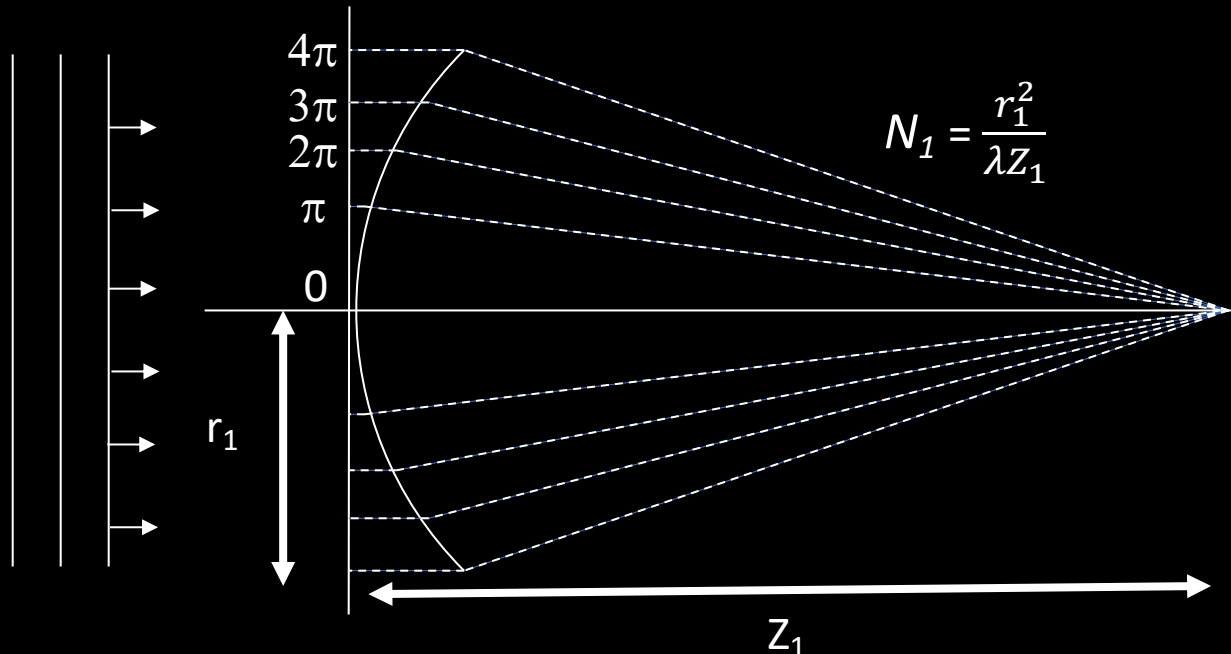
$$U(p) \propto \frac{-i}{\lambda z} \iint e^{\frac{i\pi r^2}{\lambda z}} r dr d\theta$$

Fresnel Number

$$N = \frac{r^2}{\lambda z}$$
$$\propto \frac{-i}{2} \iint e^{i\pi N} dN d\theta$$

- Same integrand
- Same integration limits relative to integrand
- Small mask has a much larger 3<sup>rd</sup> order term relative to the Fresnel approximation. Larger starshade is a better Fresnel approximation.

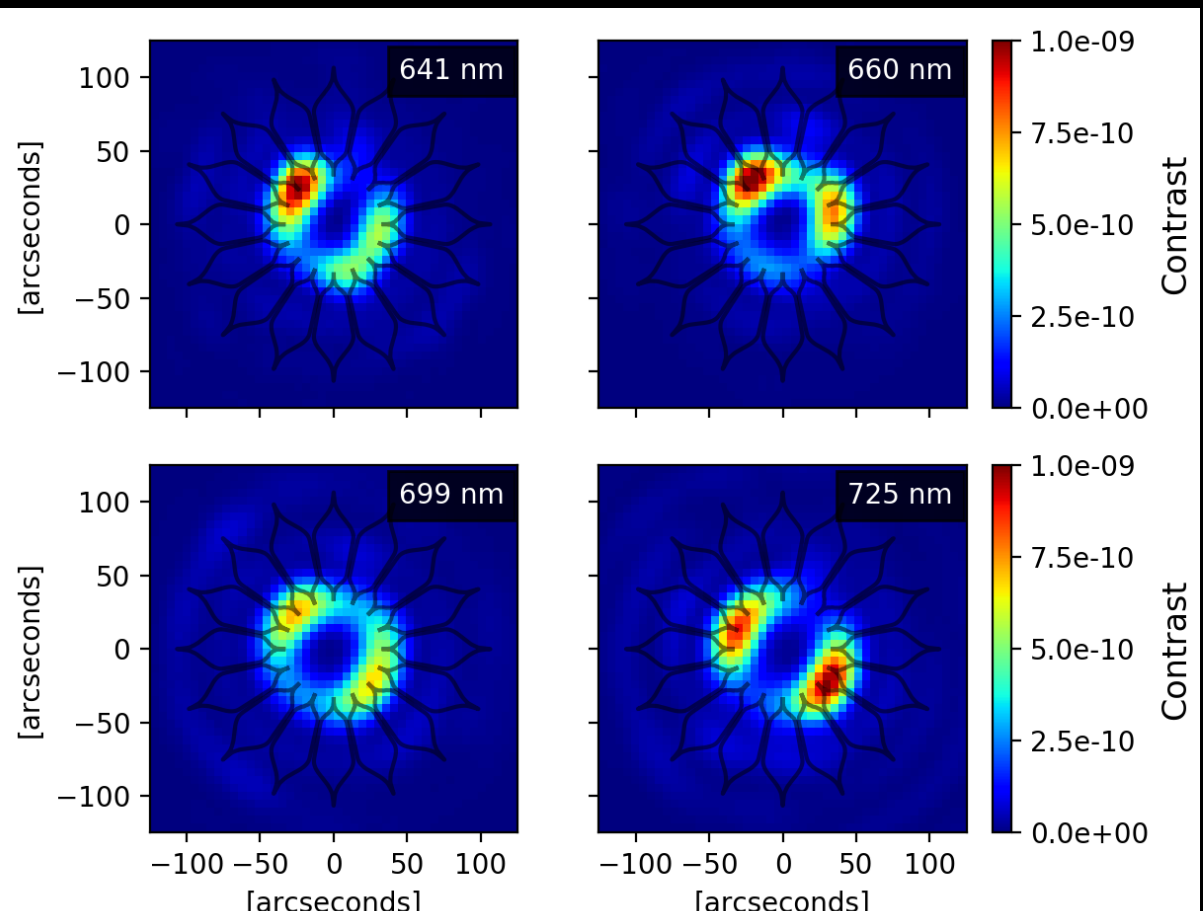
$$r_1 = .0125 \text{ m}$$
$$Z_1 = 17.76 \text{ m (eff)}$$
$$\lambda = 725 \text{ nm}$$
$$N_1 = 12.1$$
$$\text{Tel. Res} = 1.7 \lambda/D$$
$$3^{\text{rd}} \text{ order}/2^{\text{nd}} \text{ order} : 1.5\text{e-}8$$



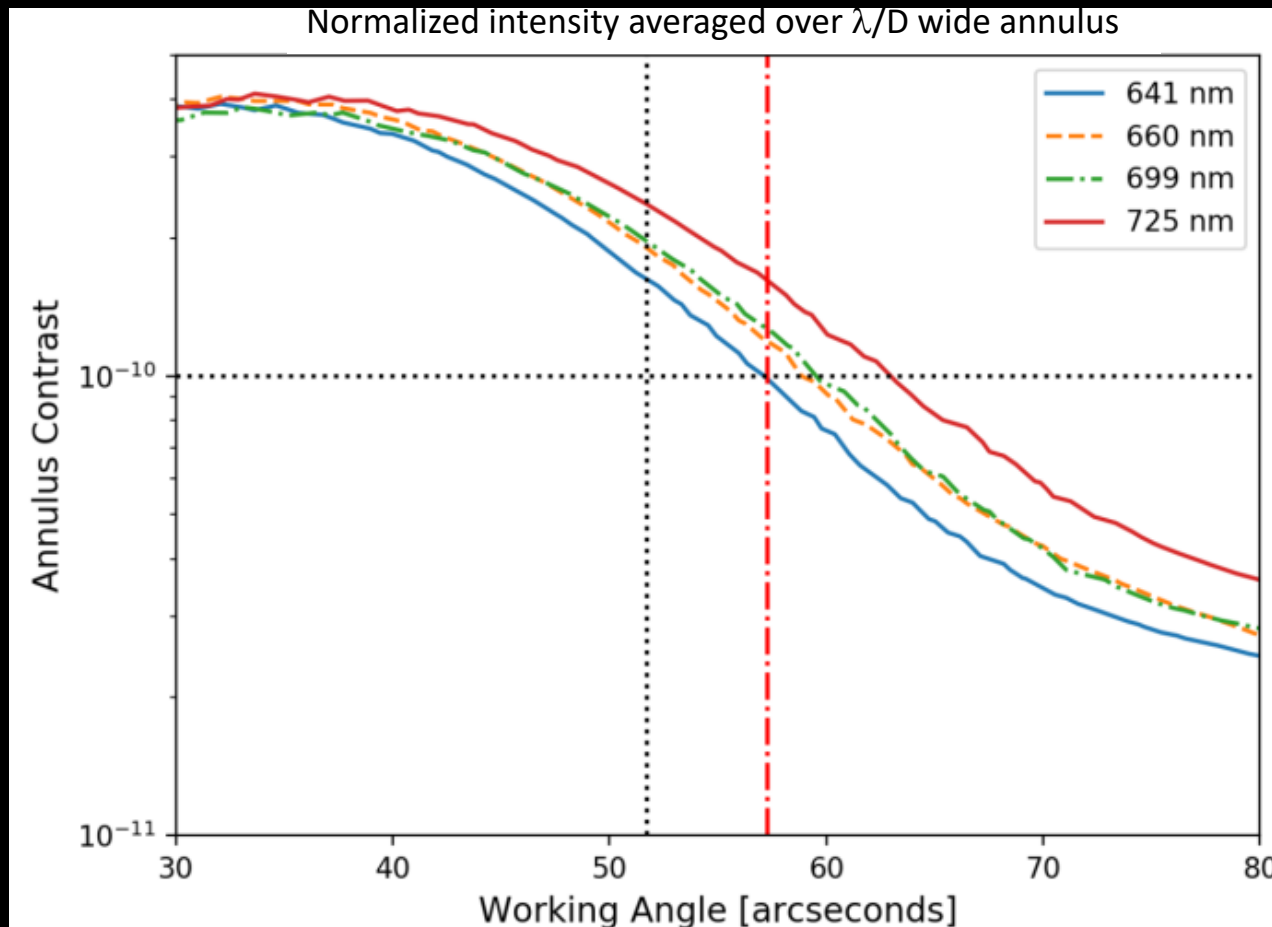
$N_1 = N_2$ : Maintaining Fresnel Number preserves the math/physics. Higher order terms are less important at large scale.

# OPTICAL TEST RESULTS: BROADBAND

4-band Results full scale



Average normalized intensity in photometric aperture



# Milestones 2: Shape Deformation Sensitivity Model Validation

**Milestone 2:** Small-scale starshade in the Princeton Testbed validates contrast vs. shape model to within 25% accuracy for induced contrast between  $10^{-9}$  and  $10^{-8}$ .

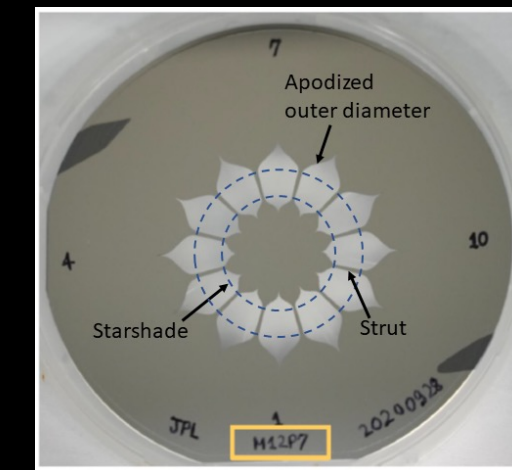
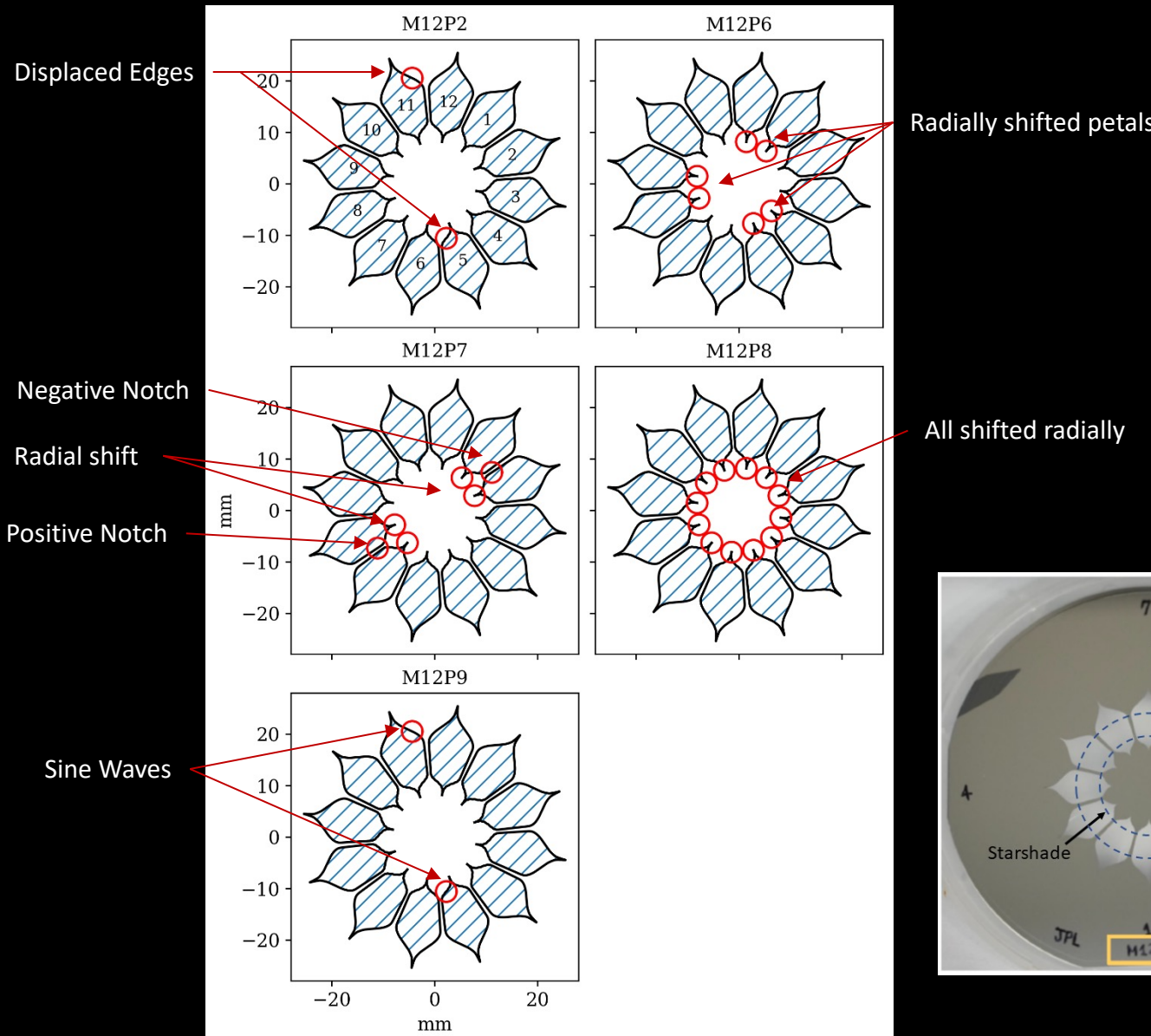
# Milestone 2 Experiment

- Introduce perturbations representative of key shape-related building blocks of the starshade instrument performance error budget
  - Petal shape: displaced edge segments
  - Petal shape: deformed petals
  - Petal position: randomly displaced petals
  - Petal position: globally displaced petals (inner disk dimension)
  - Combined errors: randomly displaced petals and displaced edge segments
  - Additionally, introduce tips in the inner starshade

Mask	Perturbation	No. Perts.
M12P2	Displaced Edges	2
M12P6+M12P10	3 Shifted Petals	3
M12P7	Shifted Petals + Displaced Edges	2
M12P8	Global Petal Shift	1
M12P9	Sine Waves	2

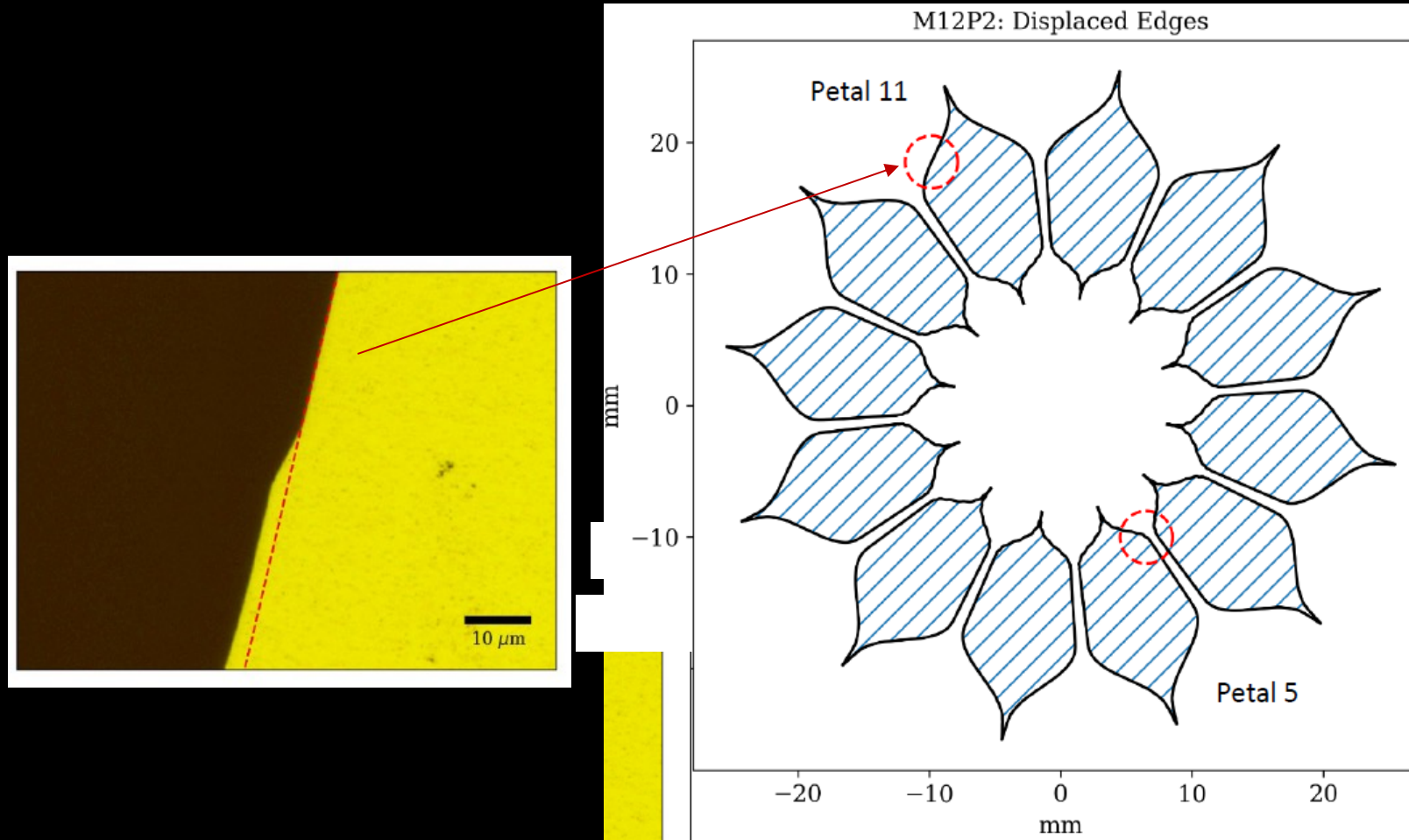
Mask M12P10 was made with the same process, approximately 1 year after M12P6.

# Shape Perturbations

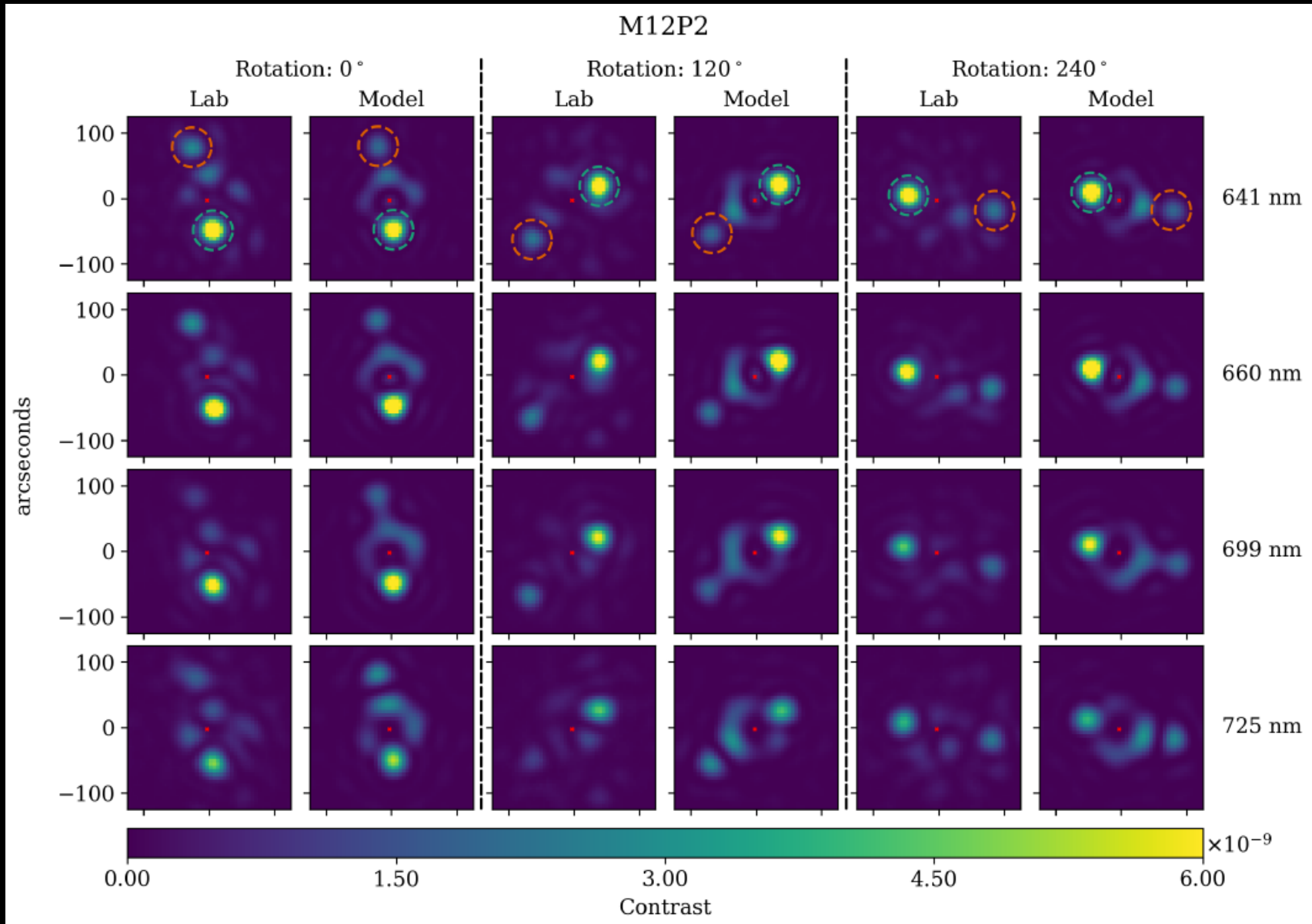


# Displaced Edge Mask

- Inner Petal 5: positively displaced edge, 3.7  $\mu\text{m}$  wide by 415  $\mu\text{m}$  long
- Outer Petal 11: positively displaced edge, 2.4  $\mu\text{m}$  wide and 530  $\mu\text{m}$  long

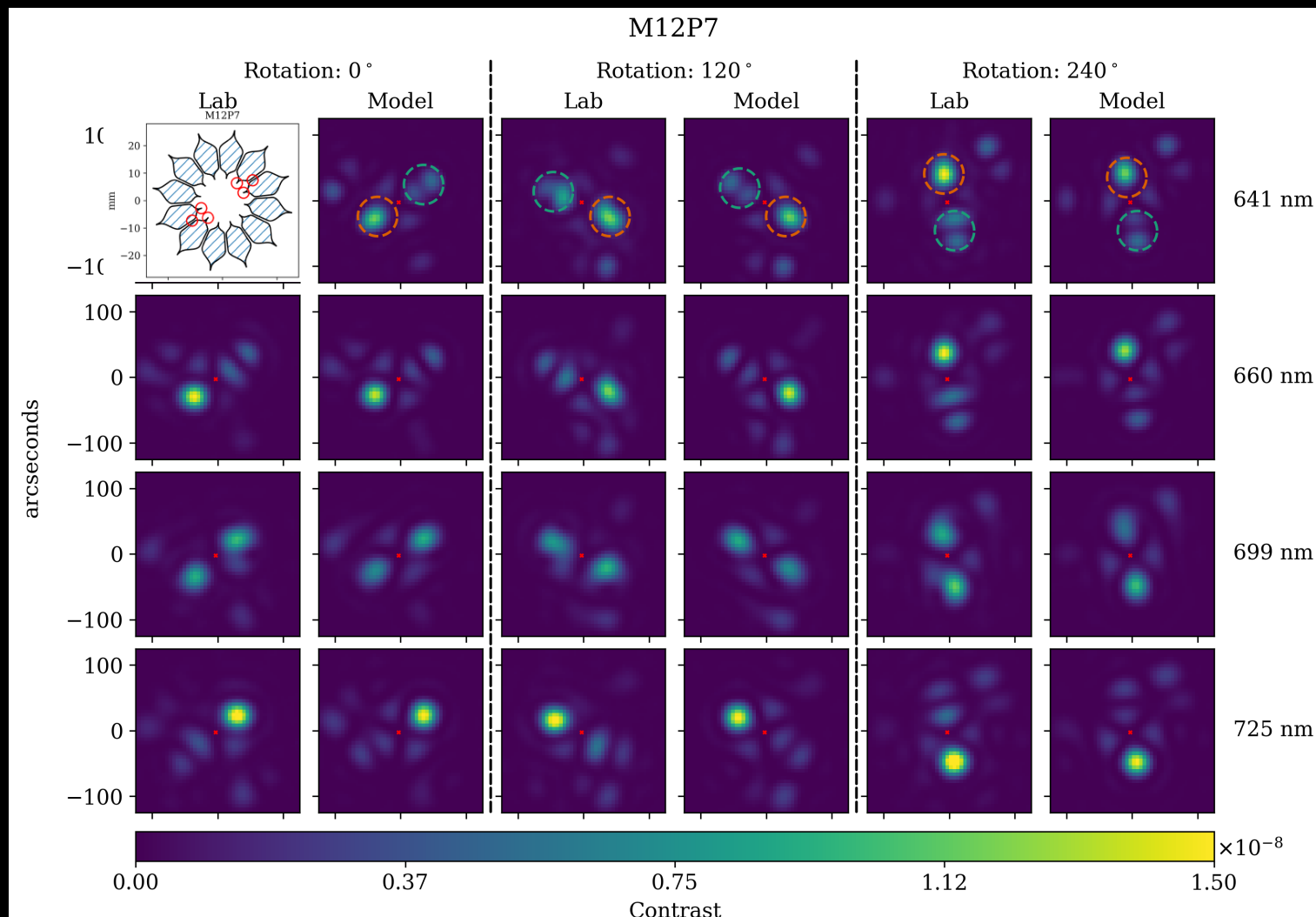


# Displaced Edge Results

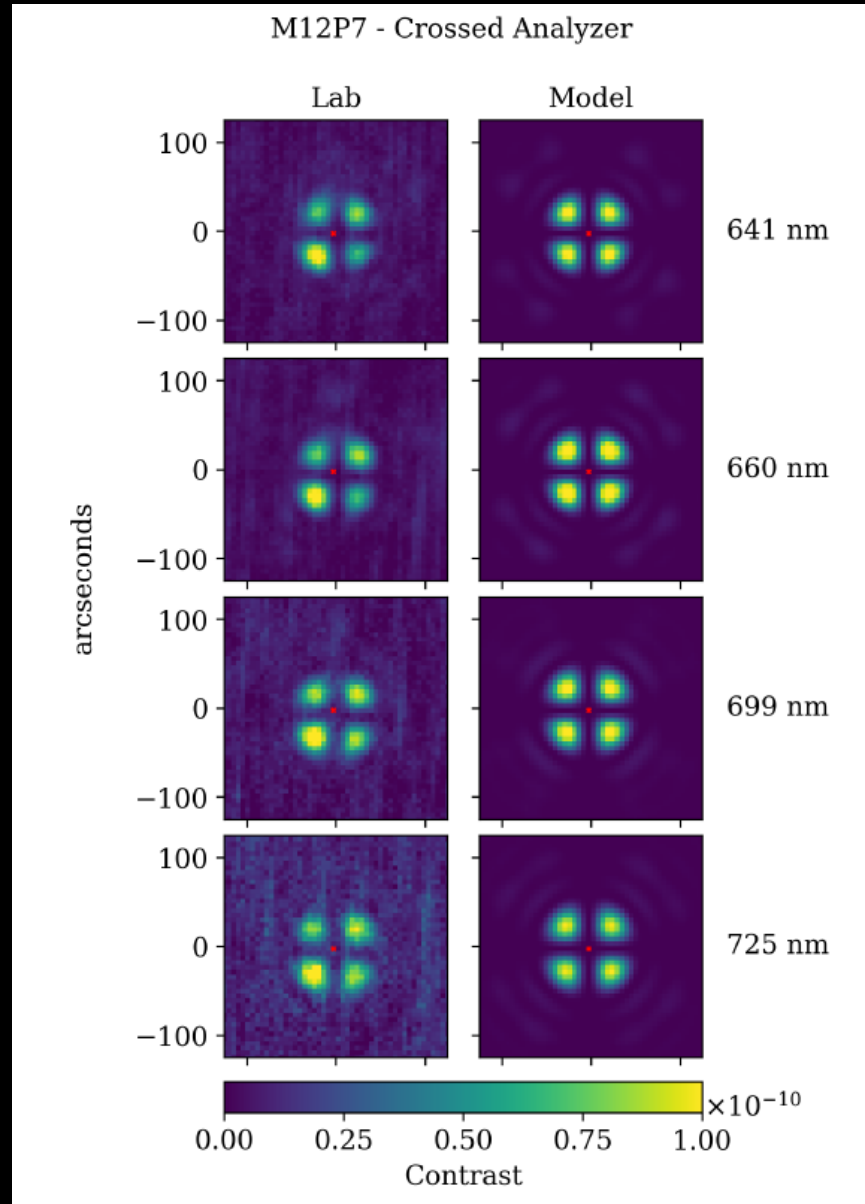


# MIXED PERTURBATION MASK

Mixed Perturbation Mask:  
2 shifted petals, two notches



# POLARIZATION LOBES: LIMITING LABORATORY PERFORMANCE



These lobes are entirely due vector diffraction at the miniature starshade edges. Models take into account sub-micron structures on the edges, material properties, polarization.

Models predict that these lobes scale with the diameter of the starshade, i.e. they will be  $10^{-16}$  contrast in a full scale starshade.

# MILESTONE 2 RESULTS: LAB AND MODEL AGREEMENT

Mask	Perturbation	Model Error*	Crossed Analyzer RMS
M12P2	Edge Notches	$-5\% \pm 5\%$	33%
M12P6 & M12P10	Shifted Petals	$94\% \pm 6\%$	15%
M12P7	Shifted Petals + Notches	$38\% \pm 11\%$	18%
M12P8	Global Shifted Petals	$23\% \pm 2\%$	49%
M12P9	Sine Waves	$0\% \pm 5\%$	33%

Recommended MUFs for Starshade Error Budget

Petal shape: 1.25

Petal Positioning: 2.0

\*

$$ME_j = \frac{\text{Lab}_j - \text{Model}_j}{\text{Model}_j} \times 100\%$$

Model error is the average for all perturbations, wavelengths, and orientations for each mask.

# RELEVANCE OF EXPERIMENT TO FLIGHT

- **Testbed is a MORE STRINGENT test of Fresnel diffraction than flight:**
  - Testbed is at flight Fresnel Number, while
  - Testbed 3<sup>rd</sup> order term is orders of magnitude greater than for flight.
  - Testbed has 2 starshades that must both work.
  - Testbed has extra edges with the struts
  - Testbed is at smaller  $\lambda/D$ .
- **Polarization limited:**
  - Experiment limited by polarization yet still has average  $2 \times 10^{-10}$  at the IWA and  $< 10^{-10}$  over 75% of search space.
  - Polarization in flight will be orders of magnitude less (ratio of area to edge length) $^2$

Demonstrated  $< 1 \times 10^{-10}$  contrast in broadband at Flight Fresnel Number and measured Model Uncertainty for Shape Perturbations.

# Milestones 4: Lateral Formation Sensing and Control

**Milestone 4:** Starshade Lateral Alignment Testbed validates the sensor model by demonstrating lateral offset position accuracy to a flight equivalent of  $\pm 30$  cm. Control system simulation using validated sensor model demonstrates on-orbit lateral position control to within  $\pm 1$  m.

# FORMATION FLYING: PRINCIPLE

The shadow is observed at wavelengths above or below the deepest shadow band. The shadow has a Spot of Arago at its center that is used for the final stage of alignment.

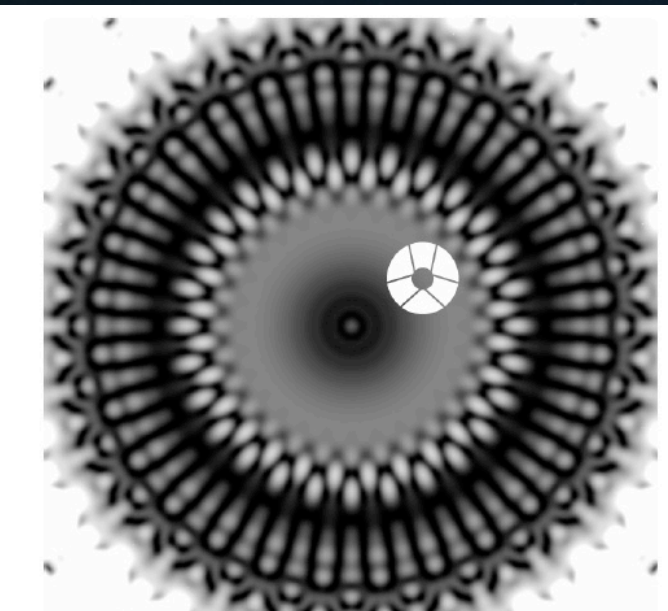
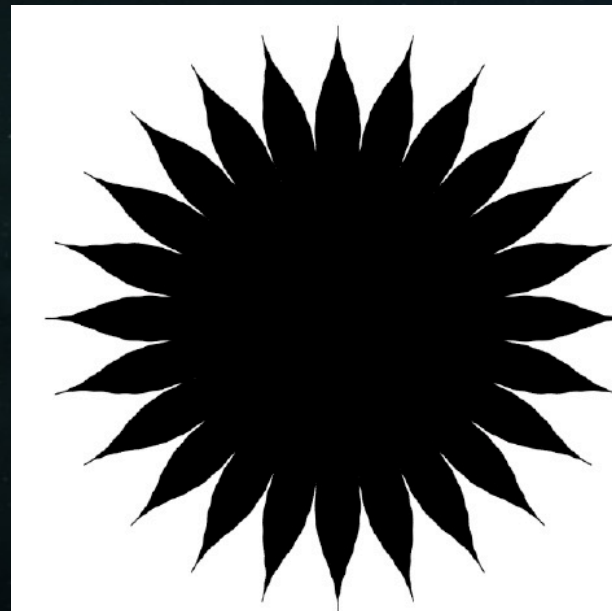
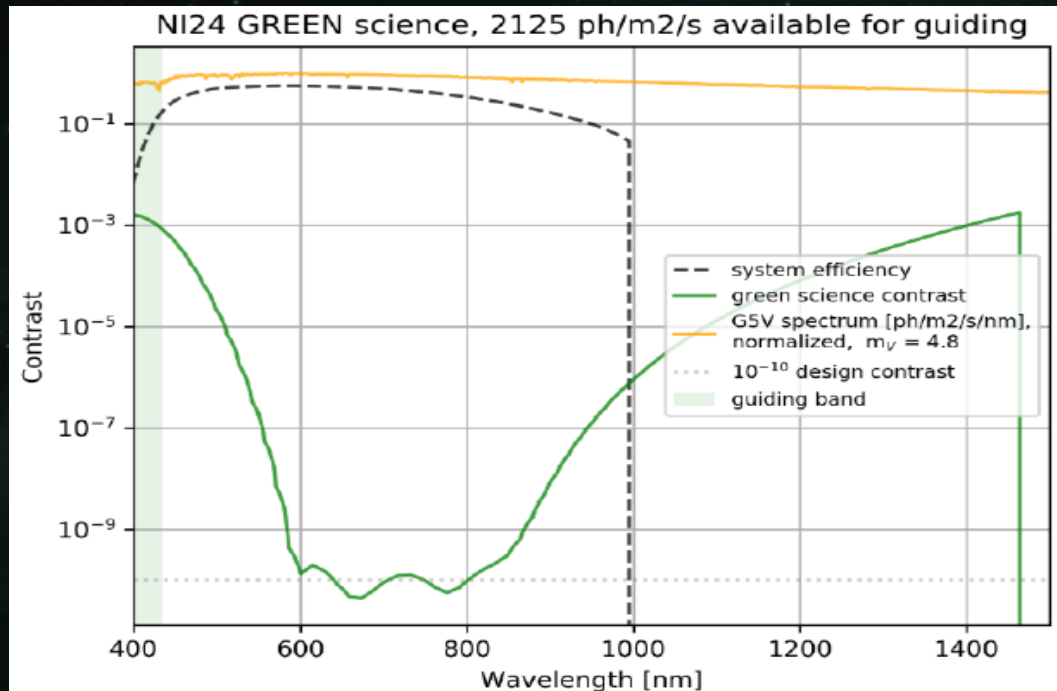
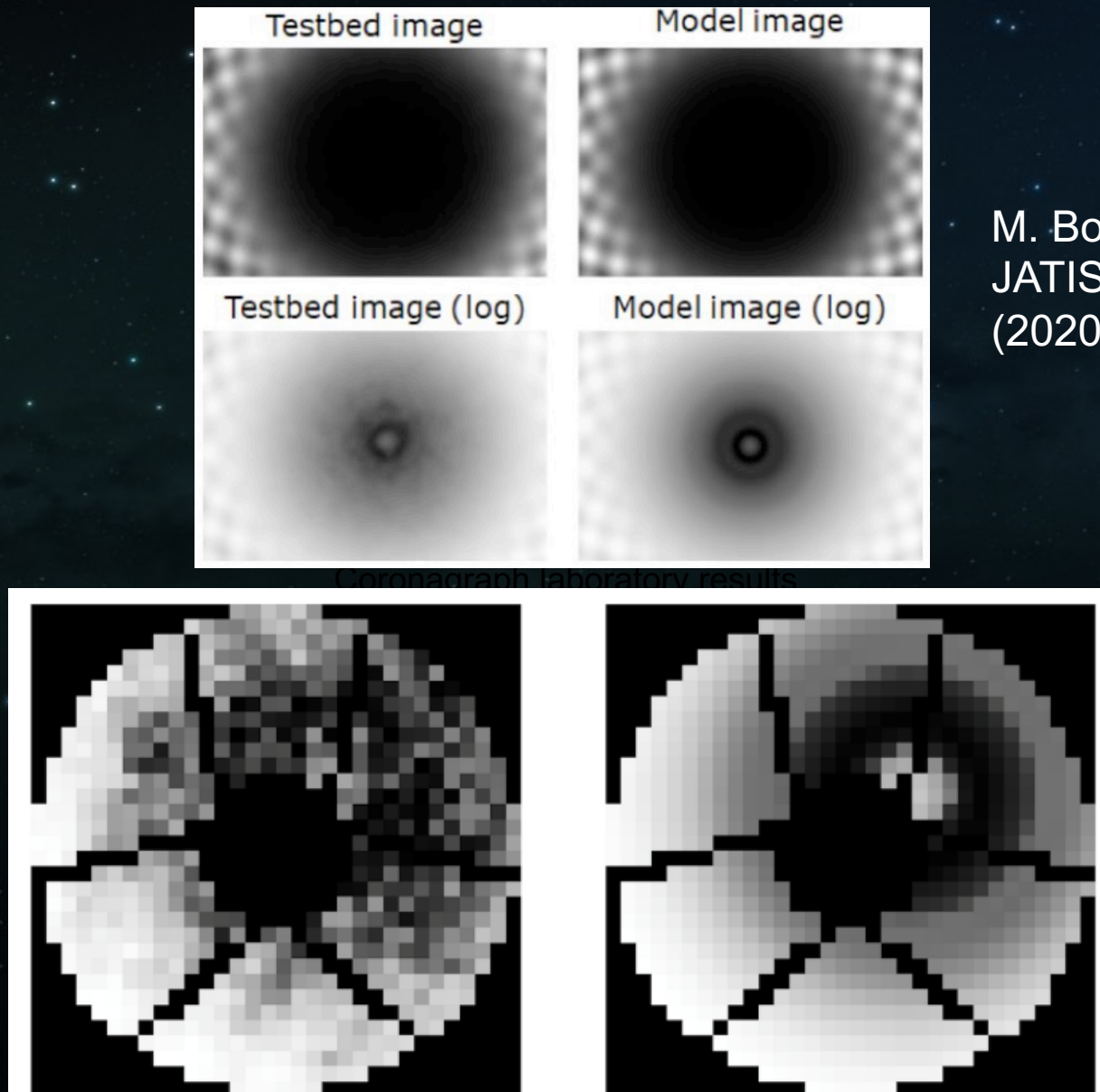
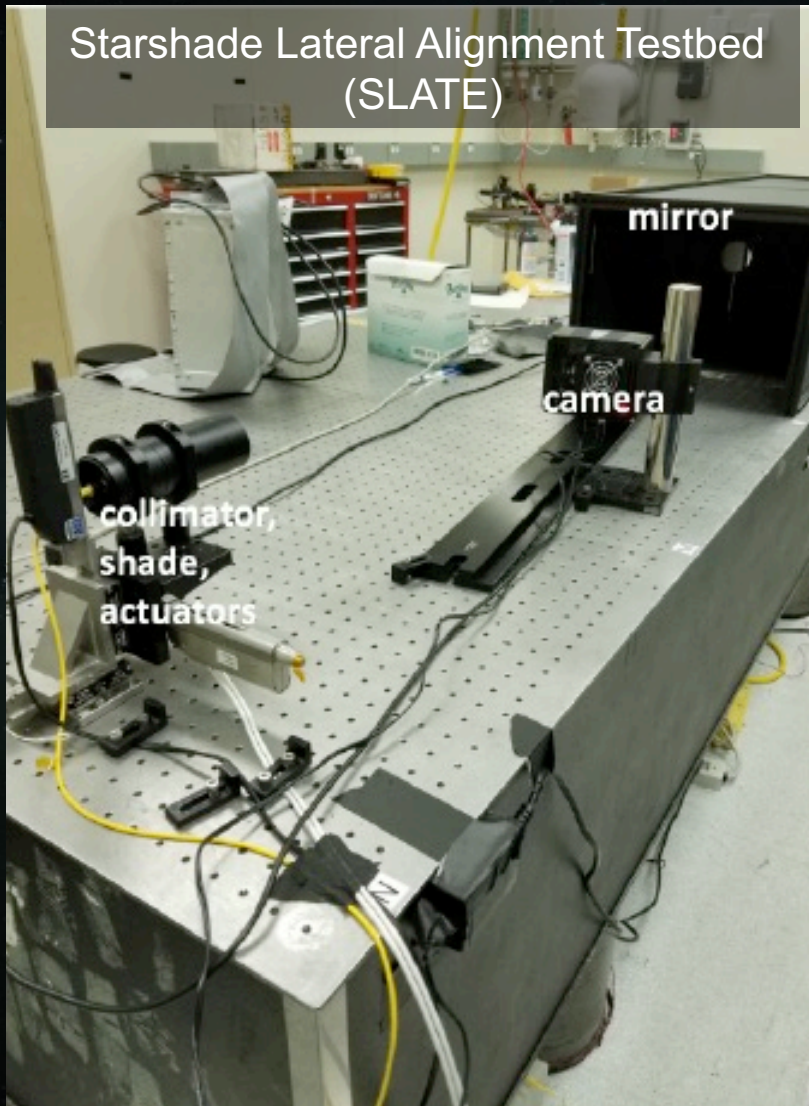


Figure 3-1: (Left) NI2-24 Starshade design (E. Cady). The Starshade is ~26 meters tip to tip. (Right) Light pattern at the location of the WFIRST telescope, stretched to show detail, with the 2.4 meter pupil shown for scale.

Starshade laboratory result

# FORMATION FLYING: TESTBED

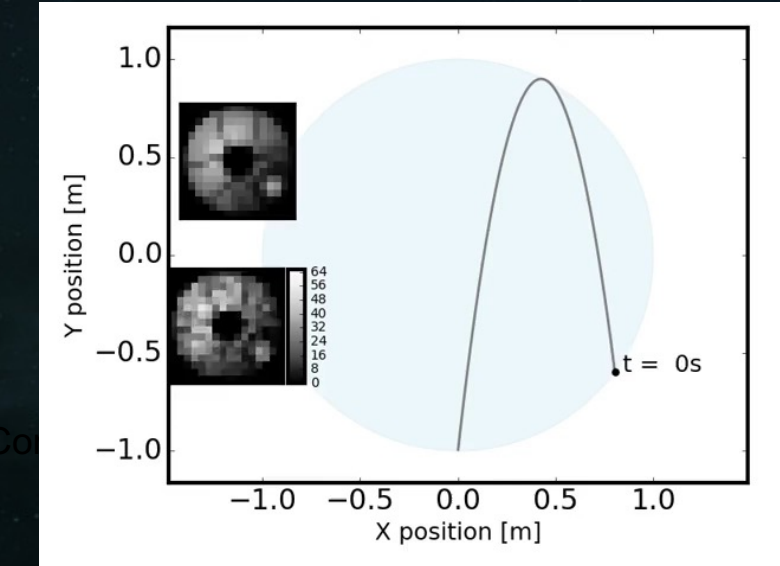
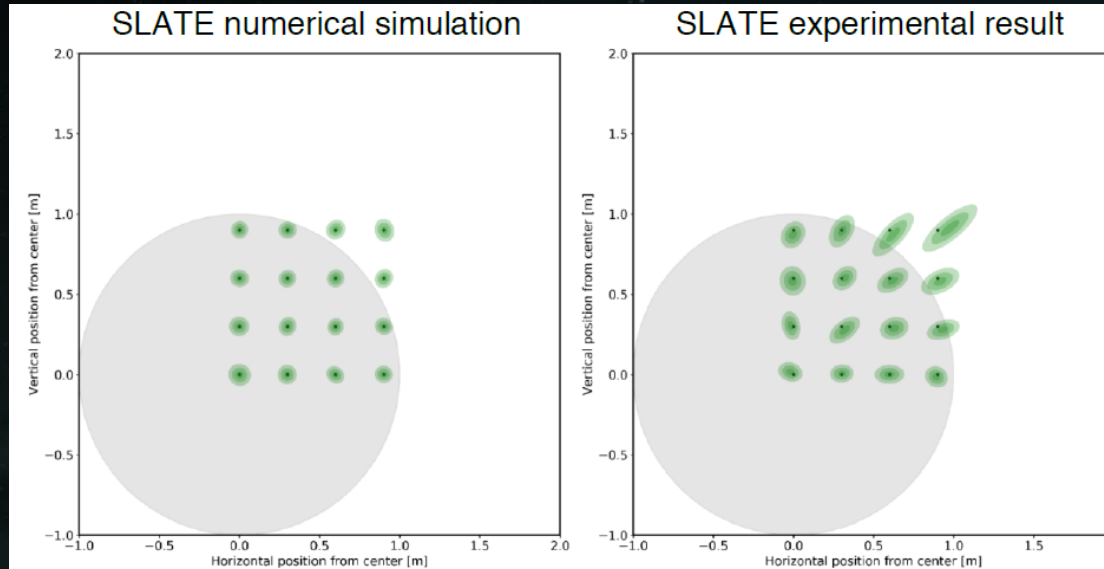


M. Bottom, et al,  
JATIS 6, 015003  
(2020).

# FORMATION FLYING: EXPERIMENTAL RESULTS

Control using a V=8 star, based on laboratory measurements and microgravity models for Starshade Rendezvous Mission.

Laboratory Results compared to model



Sim $3\sigma$ (worst)	Sim $3\sigma$ (median)	SLATE $3\sigma$ (worst)	SLATE $3\sigma$ (median)	Discrepancy (worst)	Discrepancy (median)
6.7 cm	4.0 cm	10.2 cm	6.2 cm	55%	52%

Table 3-3: Comparison between accuracy of lab-generated and simulation-based models

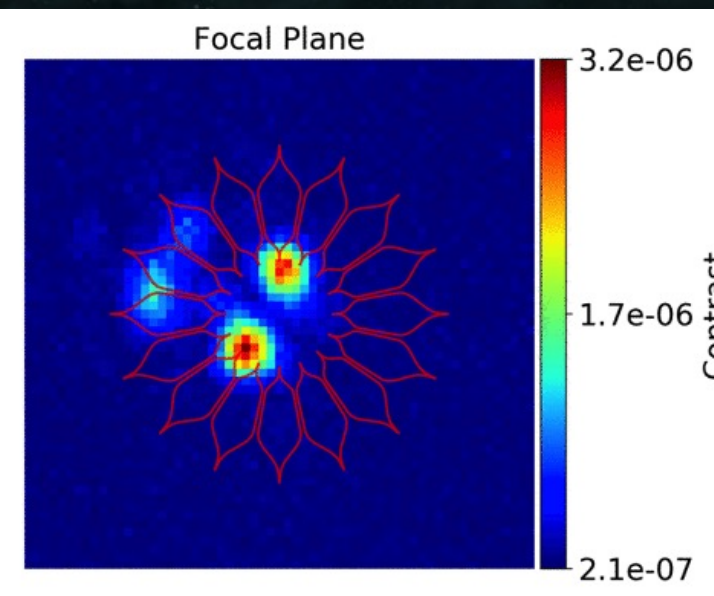
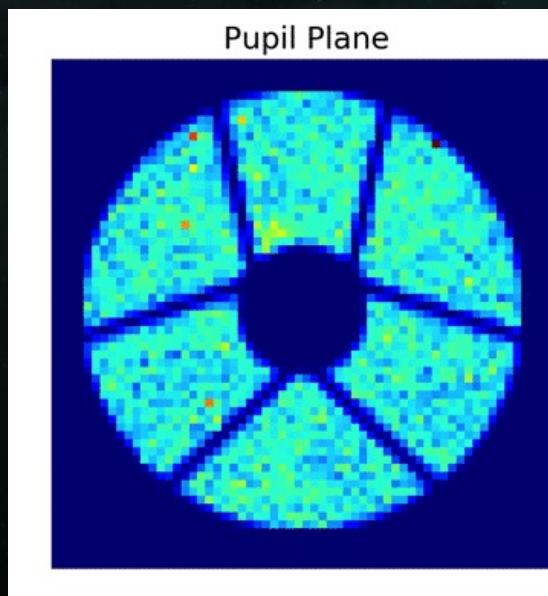
Additionally, Martin & Flinois(JATIS 014010-5, 2022) have shown that a single pupil plane sensor combined with an image-plane phase dimple mask and Neural Net provides an alternative architecture requiring one detector. Similarly, Chen, Harness, Melchoir, JATIS 2023.

# FORMATION FLYING: PRINCETON TESTBED

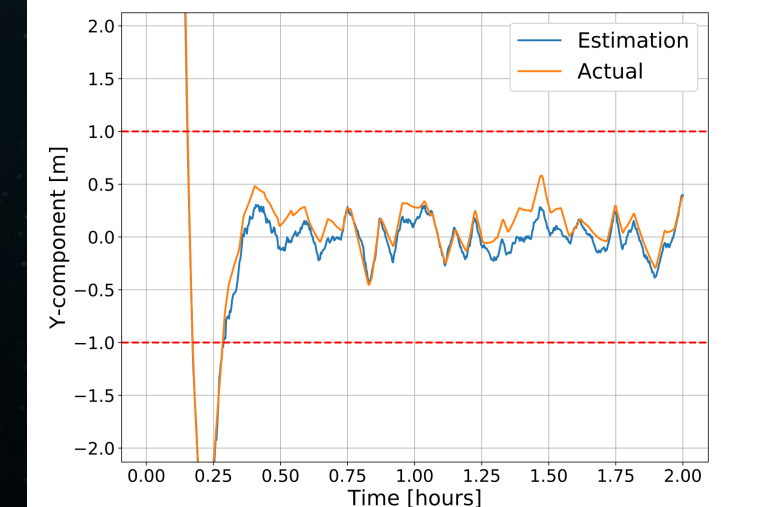
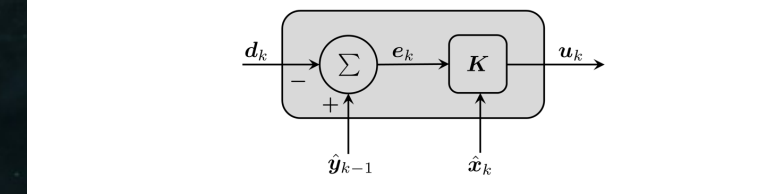
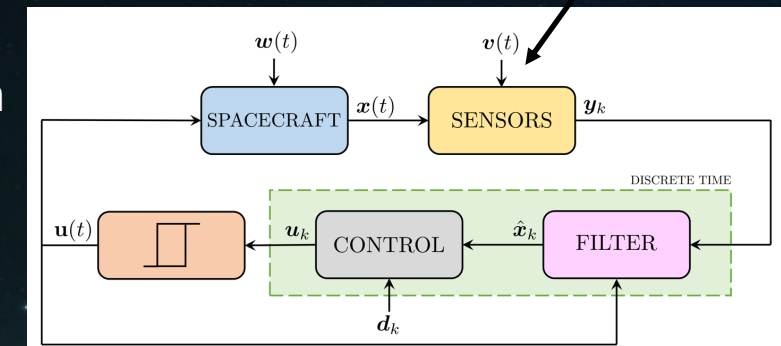
## Hardware-in-the-loop Station keeping Test

Linear Quadratic Regulator with Integral Control and Unscented Kalman Filtering

Simulated Formation keeping with actual position measurements from Princeton testbed



measure position by fitting pupil image

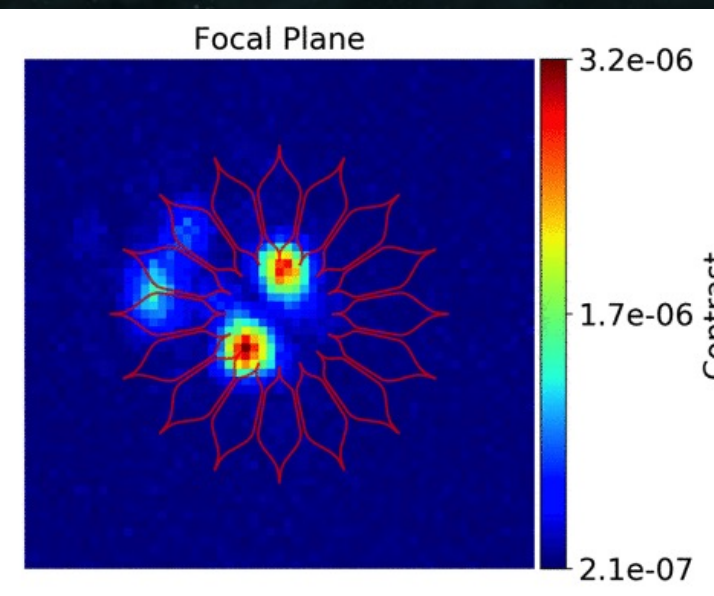
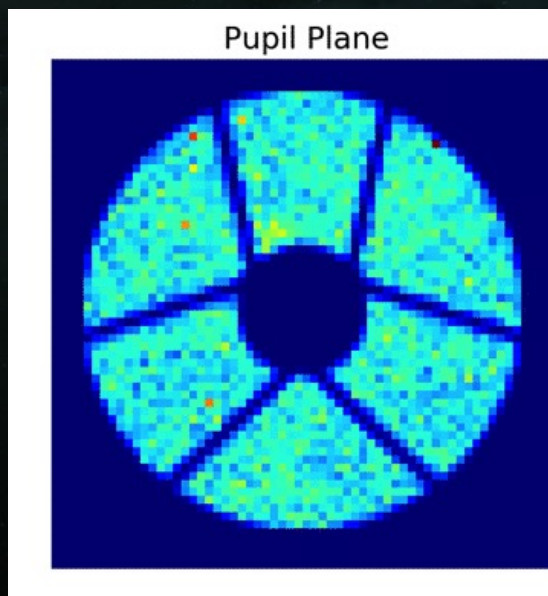


# FORMATION FLYING: PRINCETON TESTBED

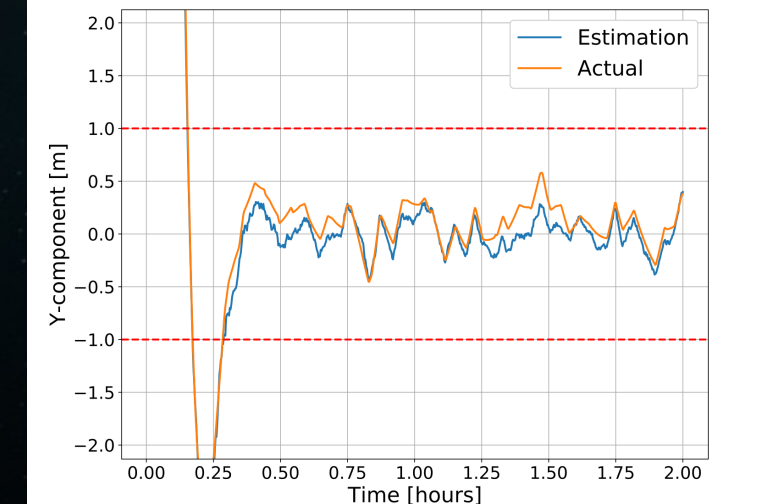
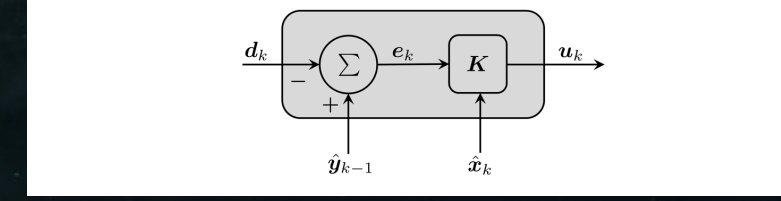
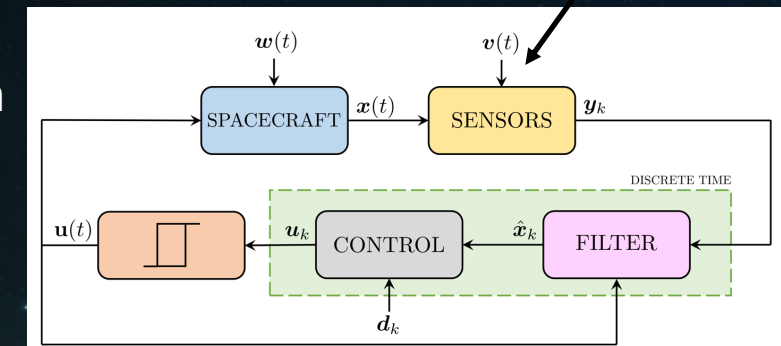
Hardware-in-the-loop Station keeping Test

Linear Quadratic Regulator with  
Integral Control and Unscented  
Kalman Filtering

Demonstrated formation keeping with actual position  
measurements from Princeton testbed



measure position by  
fitting pupil image



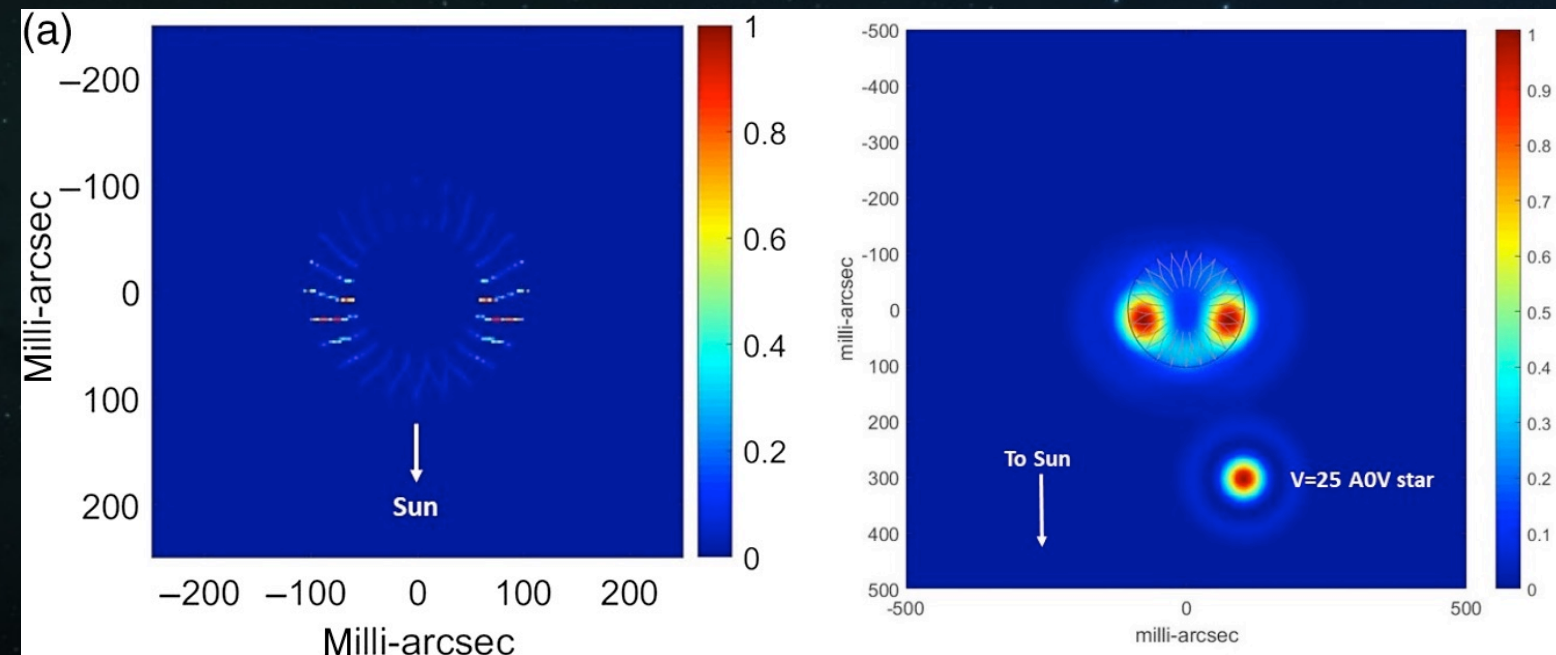
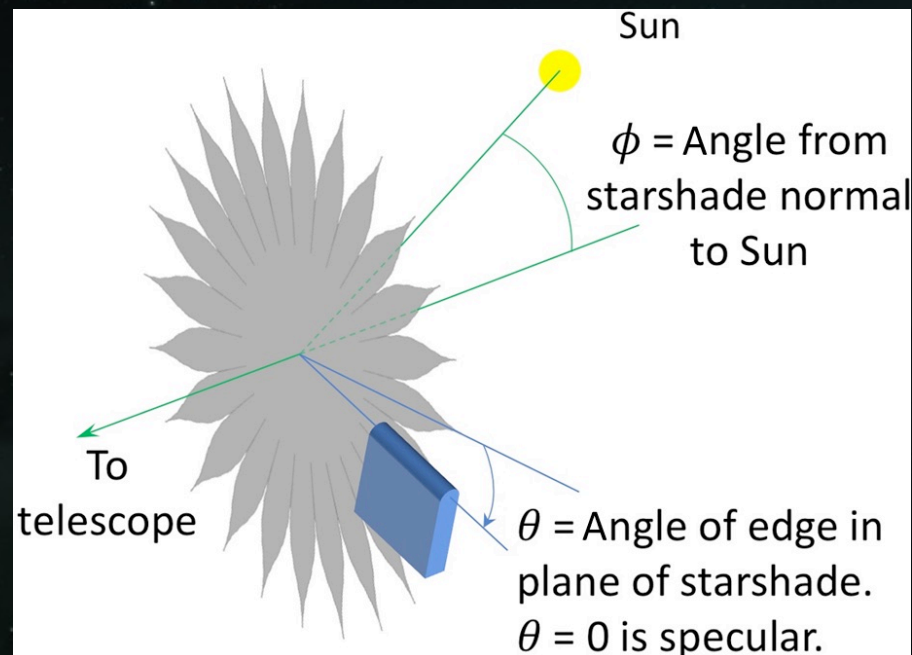
# MILESTONES 3: DEMONSTRATION OF SOLAR GLINT LOBE SCATTER PERFORMANCE

**Milestone 3:** Optical edge segments demonstrate scatter performance consistent with solar glint lobes fainter than visual magnitude 25 after relevant thermal and deploy cycles.

# MILESTONES 3: EXPERIMENTS, INCLUDING POST-MILESTONE

- Uncoated edges
  - Measure edge coupons: determine 3-D scattering characteristics
  - Measure edge segments: determine scattering behavior over
  - Model scatter using FDTD codes (MEEP, Lumerical)
  - Incorporate scatter measurements into starshade imaging s/w (SISTER)
- Coated edges
  - Formulate coatings (few-layer, metal/dielectric), coat edges (Zecoat Inc.), update models
  - Measure scatter performance
  - Tolerance coating designs
- Particulate Contamination
  - Contaminate surfaces and edges, measure edge scatter
  - Develop model linking surface contamination to edge contamination
  - Develop surface contamination requirements to ensure edge scatter performance requirements are met.

# SOLAR EDGE SCATTER GEOMETRY



# SCATTEROMETERS

We designed and built two scatterometer to measure edge scatter:

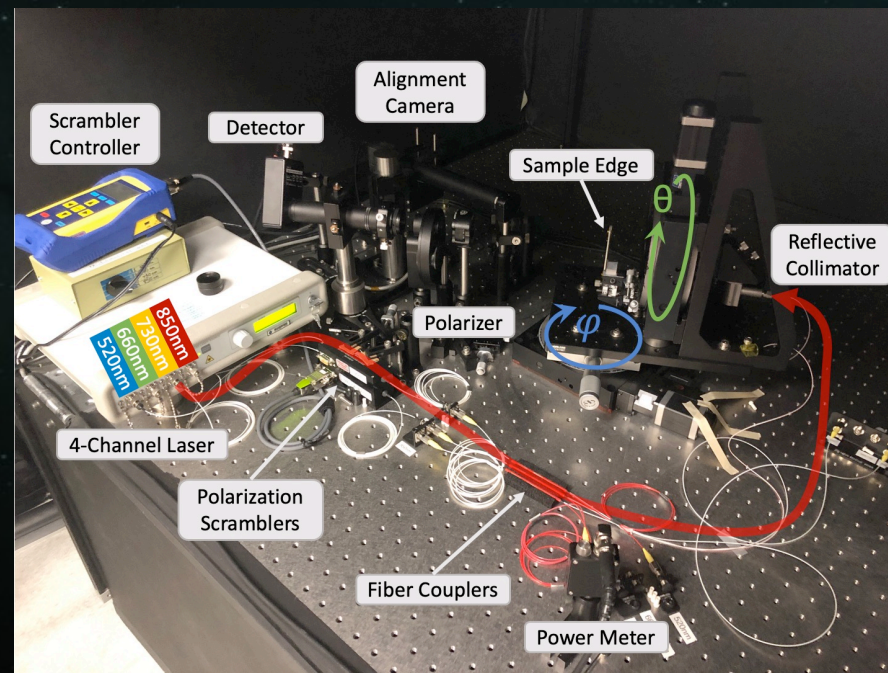
## Multi-Angle Scatterometer (MAS)

BRDF for edge coupons

Measures reflectivity in orthogonal polarizations

3 mm diameter spot on the sample

Ultimately modified to measure 4 wavelengths



McKeithen et al, Proc. SPIE 11443 (2020).

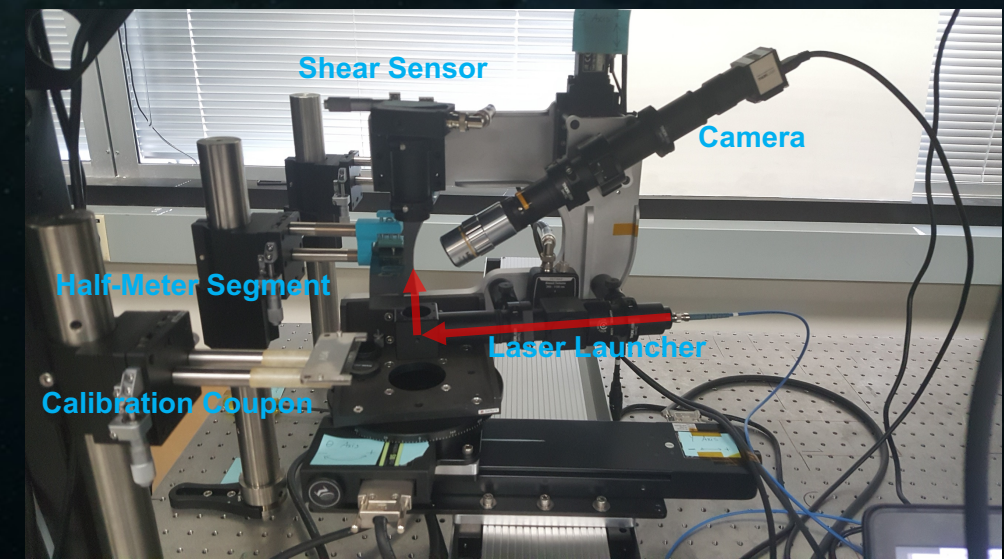
## Single-Angle Scatterometer (SAS)

Fixed wide-angle ( $30^\circ$ ) sensor

Scans along 1-m curved edge

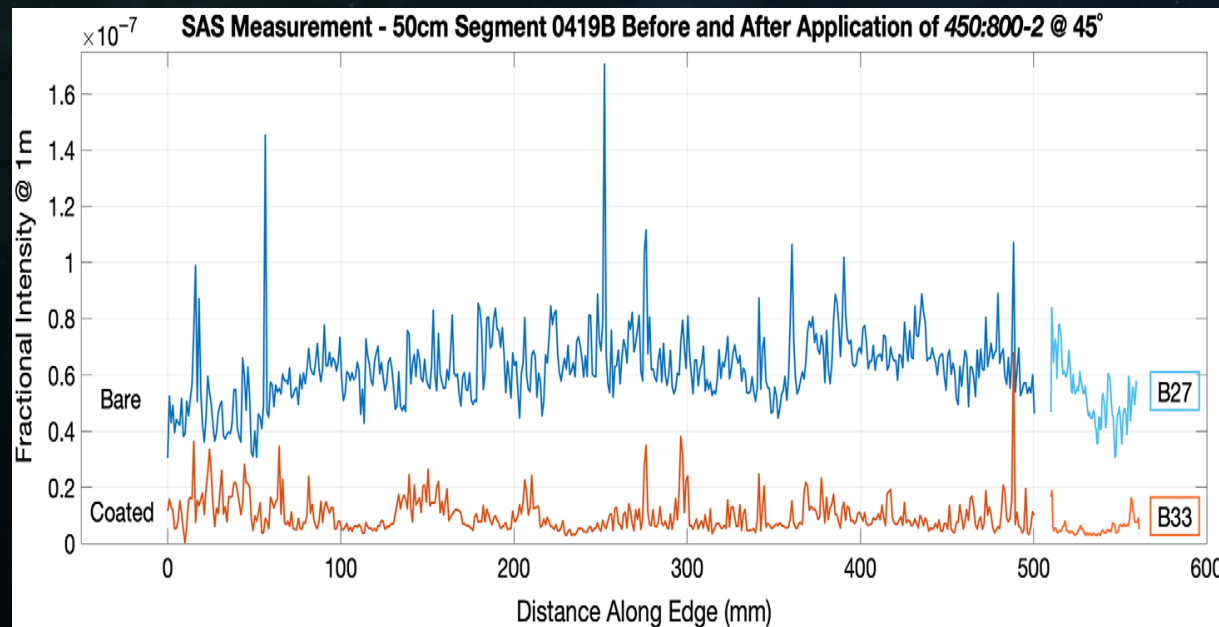
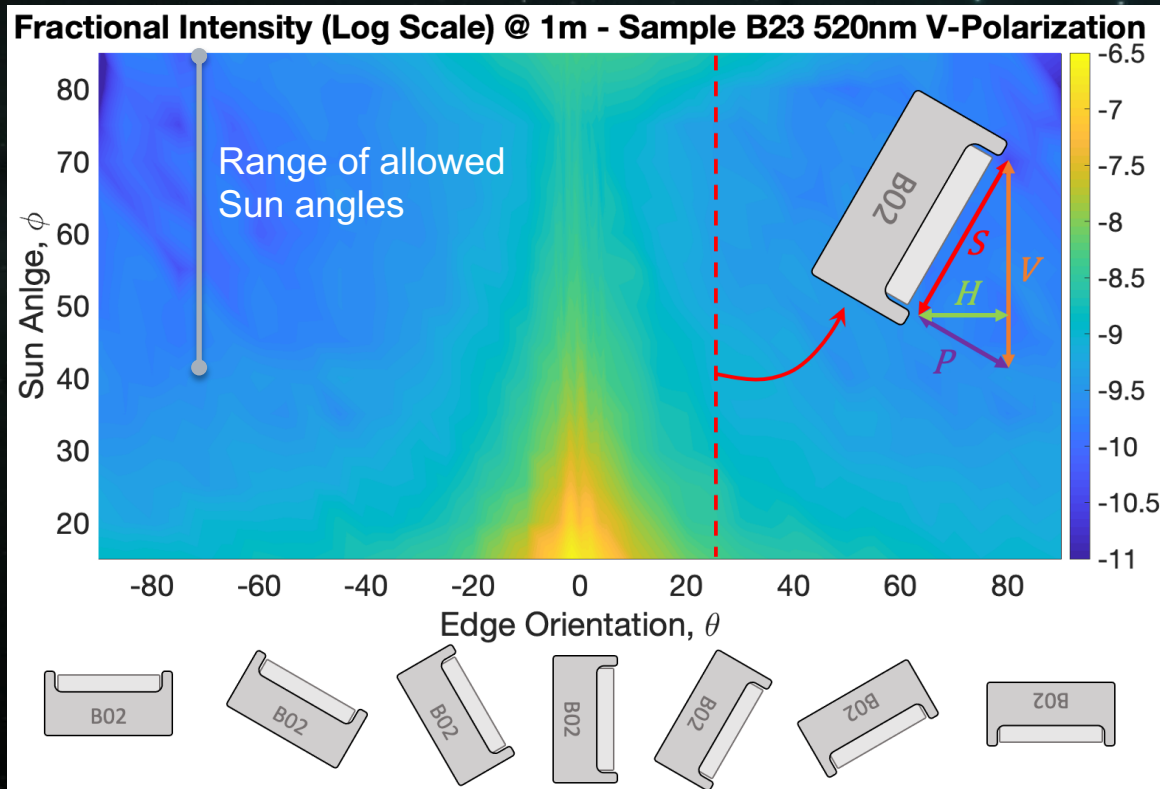
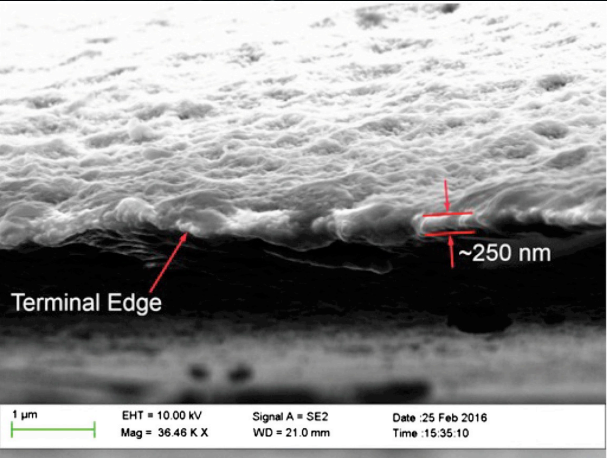
10 micron resolution

633 nm



Shaklan et al, JATIS vol 7 (2021)

# COUPONS AND EDGE SEGMENTS



# OPTICAL EDGE SCATTER RESULTS

HabEx 300-1000 SRM 615-800 SRM 425-552

**Table 3** Estimated glint lobe magnitude in Roman Space Telescope Rendezvous 425- to 552-nm band.

Lobe	$r > \text{IWA}$	IWA phot.	IWA phot.	IWA phot.	
$\phi$	mag <sup>a</sup>	mag <sup>b</sup>	min. mag <sup>c</sup>	Avg. mag <sup>d</sup>	95% conf. <sup>e</sup>
53	25.8	26.8	26.7	27.6	27.3
63	25.9	26.9	26.9	27.7	27.5
73	25.7	26.7	26.7	27.5	27.3
83	25.2	26.2	26.2	27.0	26.7

$\phi$	mag	mag	min. mag	Avg. mag	95% conf.
53	23.7	24.7	24.6	25.5	25.2
63	23.8	24.9	24.8	25.6	25.4
73	23.6	24.7	24.6	25.4	25.2
83	23.1	24.1	24.1	24.9	24.6

$\phi$	mag	mag	min. mag	Avg. mag	95% conf.
35	25.0	26.4	26.4	27.5	27.2
45	25.6	27.0	27.1	28.1	27.8
55	25.9	27.3	27.4	28.4	28.1
65	26.0	27.4	27.5	28.4	28.2
75	25.8	27.1	27.3	28.2	27.9
85	25.2	26.6	26.7	27.6	27.3

**Table 6** Estimated glint lobe magnitude for optimized, as-manufactured coatings.

$\phi$ (deg)	IWA phot. 95% conf.	Improvement ratio	$\Delta\text{Mag}$	Final mag
SRM 425 to 552 nm band				
53	27.3	9.2	2.4	29.7
63	27.5	16.7	3.1	30.6
73	27.3	26.8	3.6	30.9
83	26.7	20.5	3.3	30.0

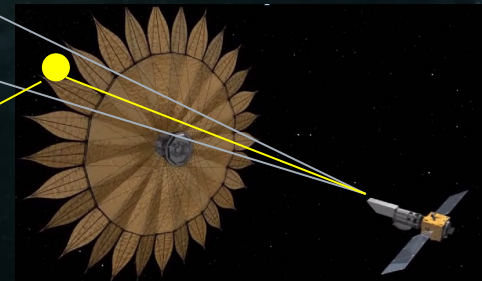
$\phi$	IWA phot. 95% conf.	Improvement ratio	$\Delta\text{Mag}$	Final mag
SRM 615 to 800 nm band				
53	25.2	14.3	2.9	28.1
63	25.4	33.3	3.8	29.2
73	25.2	61.0	4.5	29.7
83	24.6	85.3	4.8	29.4

$\phi$	IWA phot. 95% conf.	Improvement ratio	$\Delta\text{Mag}$	Final mag
HabEx 300 to 1000 nm band				
35	27.2	4.0	1.5	28.7
45	27.8	6.7	2.1	29.9
55	28.1	11.2	2.6	30.7
65	28.2	17.3	3.1	31.3
75	27.9	23.1	3.4	31.3
85	27.3	27.4	3.6	30.9

# OPTICAL EDGE CONTAMINATION



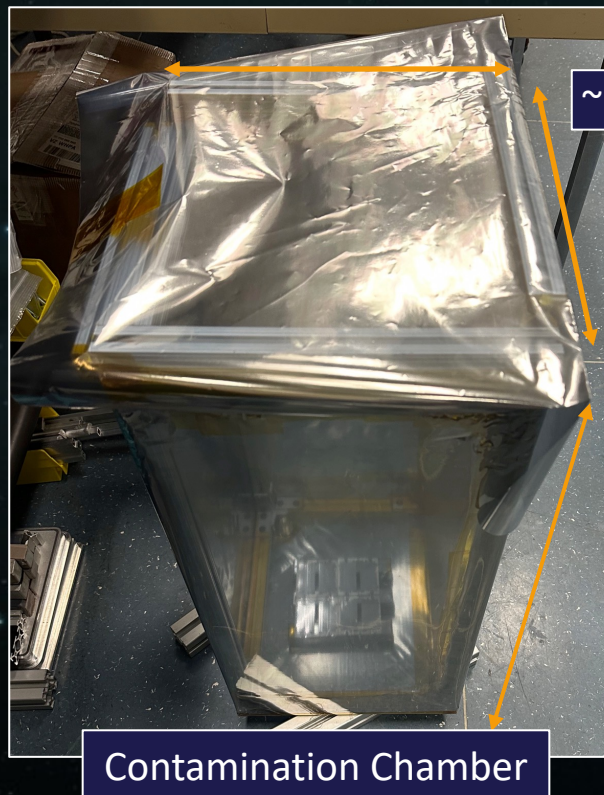
An Earth-size planet at 10 parsecs projects as a 1 mm diameter particle on the edge of the Rendezvous starshade.



$1 \text{ mm}^2$  is equivalent to 10,000 particles of dust 10  $\mu\text{m}$  in diameter, spread over about 100 m of the starshade edge.  
*Is this a problem?*

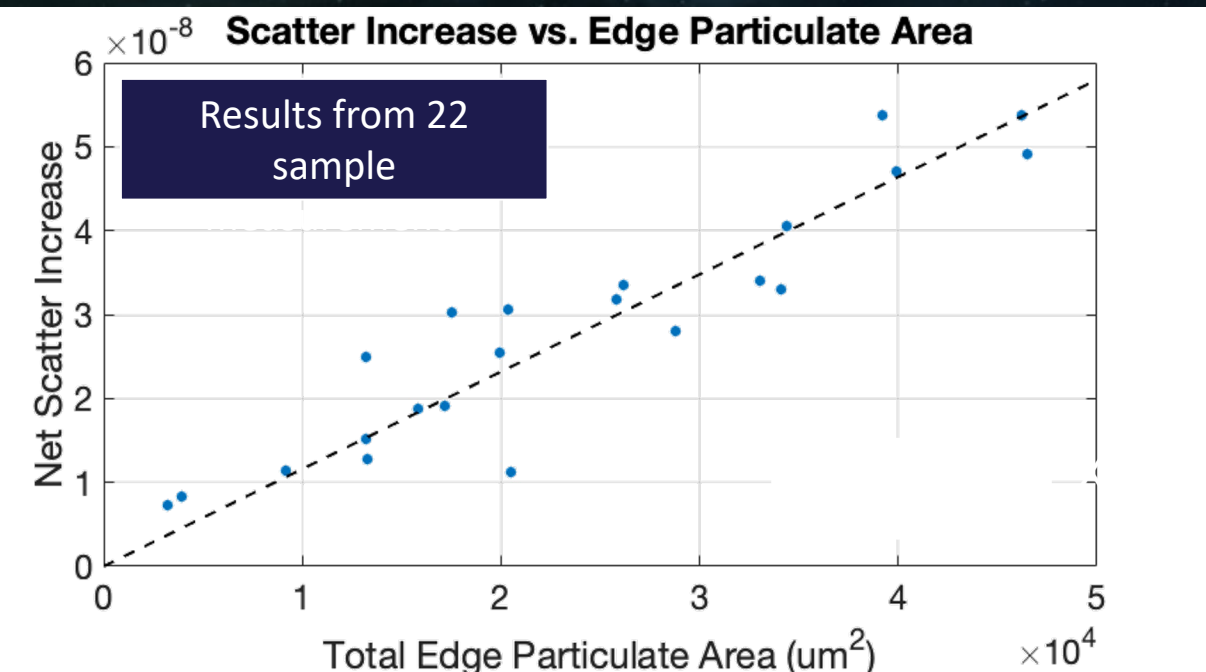
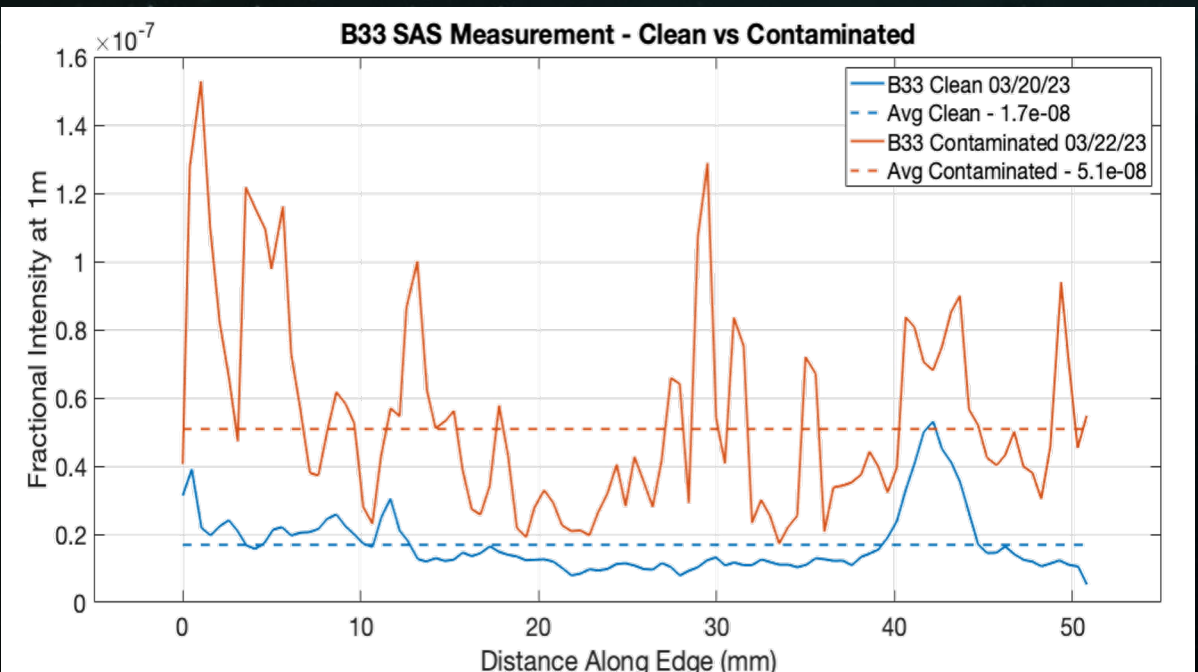
# EDGE CONTAMINATION: EXPERIMENT

We studied the scatter from particulates that can contaminate the starshade's sharp edge. With almost no literature on edge contamination, we developed a relationship between surface contaminants and edge contaminants.  
*McKeithen et al, SPIE 2023.*



# EDGE CONTAMINATION: SCATTER CHARACTERIZATION

Edge scatter is measured before and after contamination using the Single-Angle Scatterometer (SAS)  
Scatter increase is directly correlated with edge contamination

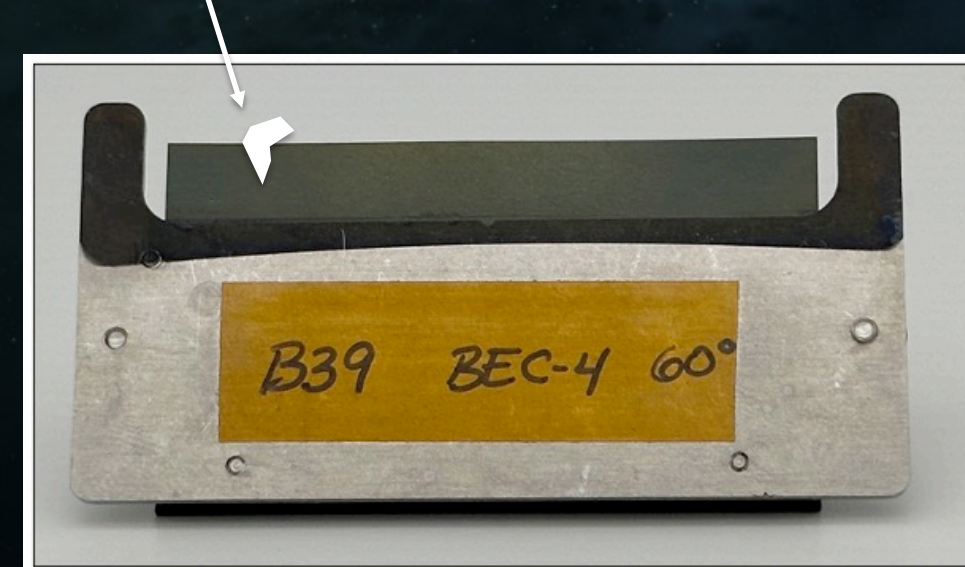


# EDGE CONTAMINATION: CALIBRATION OF SURFACE VS. EDGE

We used a calibration mask, with mask coupons lithographically placed on glass, to emulate the free-space coupons. This allows us to compare surface / edge particle density ratios and to identify edge effects, as illustrated below.

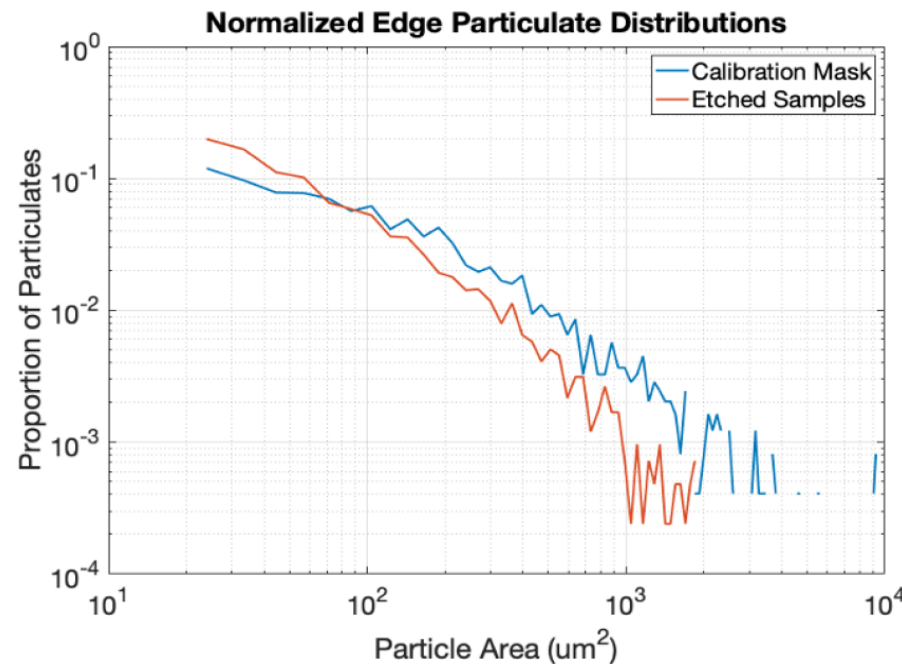


Dust particle lands here and can fall off.

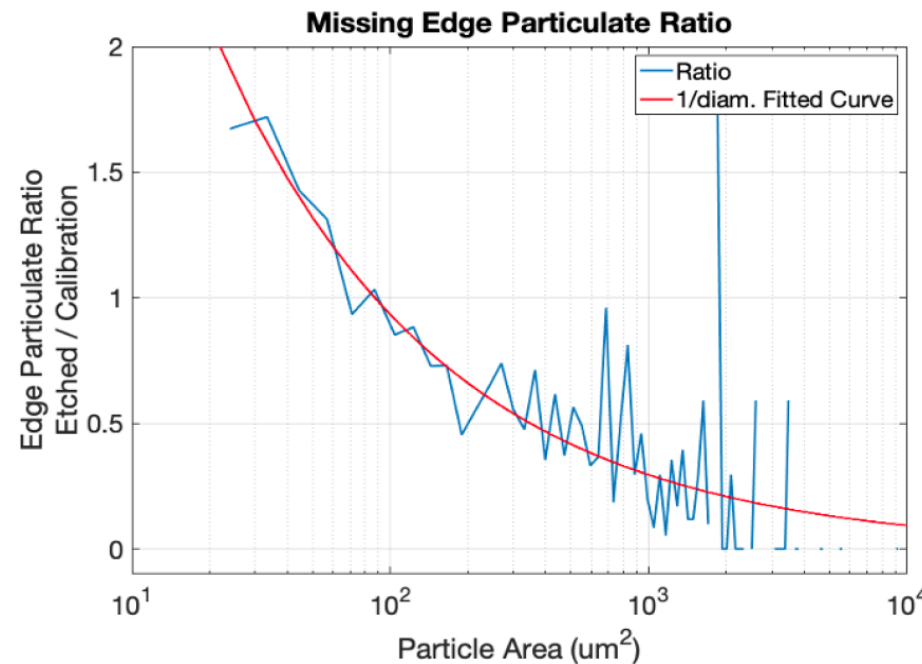


# EDGE CONTAMINATION: SURFACE VS. EDGE RESULTS

We found that the coupons were missing particles, in proportion to  $1/\text{Diameter}$ , compared to the calibration mask. Why? We are not sure, but we refer to the  $1/\text{D}$  correction as an ‘adhesion factor.’



(a)

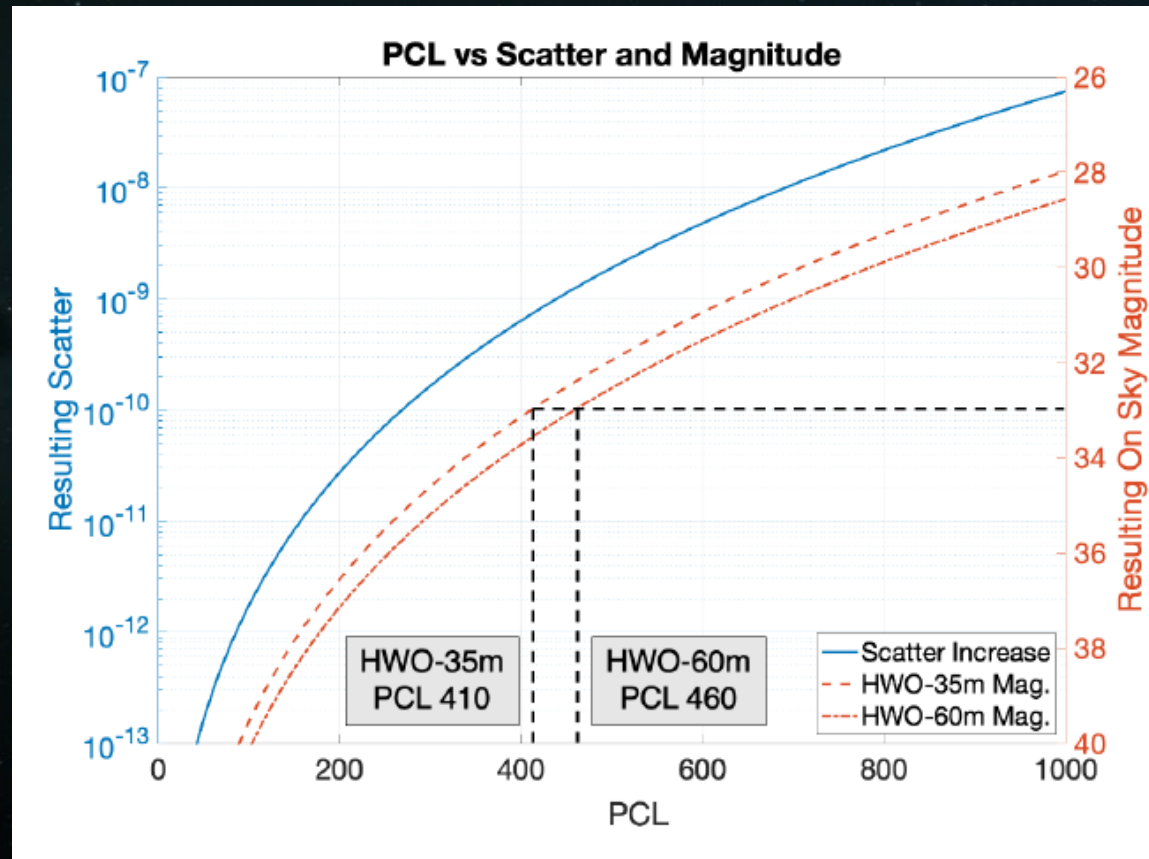


(b)

Figure 16. (a) Normalized edge particulate distributions for the calibration mask and the etched samples. Each distribution has been normalized based on the total number of edge particulates. (b) Ratio of the normalized edge distributions, representing the portion of particulates missing from the etched samples. The ratio decreases with particulate size inversely proportional to the particle diameter.

# EDGE CONTAMINATION: REQUIREMENTS

Using the experimental relationship between edge scatter and surface contamination, we derived surface contamination requirements specified in terms of standard Particle Contamination Level (PCL).



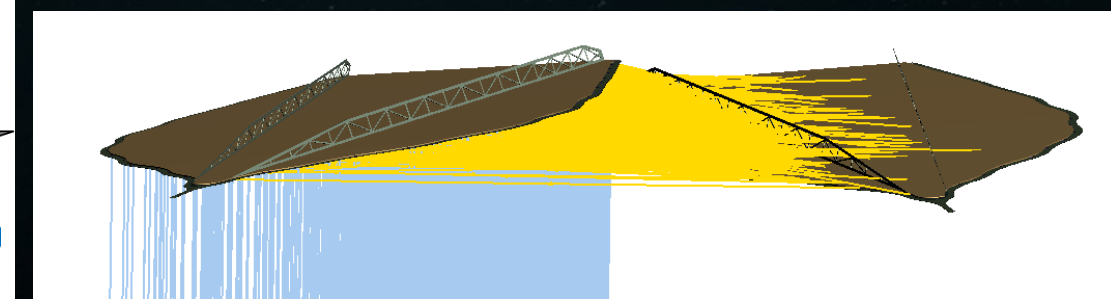
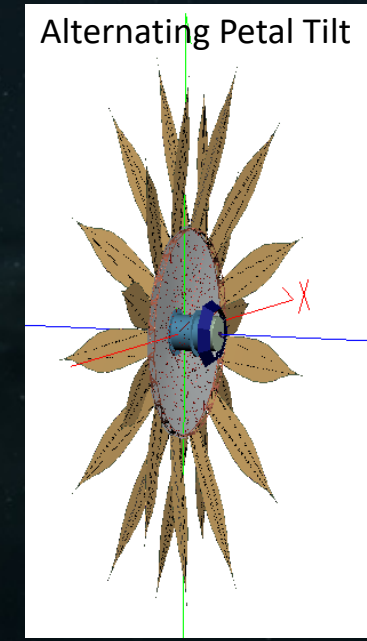
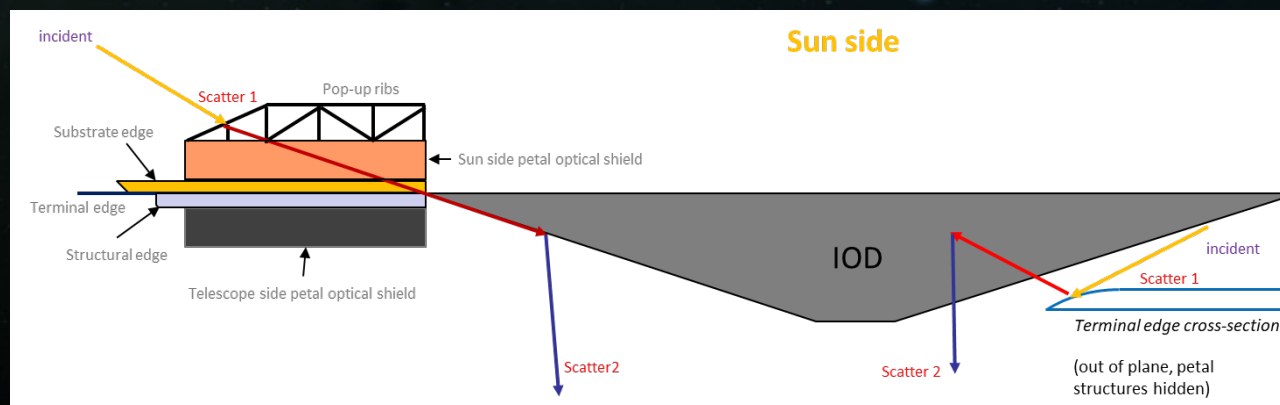
PCL 410 is ~ 0.1% particle area coverage (for slope = -.926).

PCL 460 is ~ 0.2% particle area coverage (for slope = -.926).

# STRAY LIGHT (OTHER THAN SINGLE EDGE SCATTER)

The starshade is designed so that there are no specular ray paths from the Sun to the telescope, except, unavoidably, at the petal edges. Non-specular paths with multiple bounces exist and have been extensively modeled.

- Modeled 26 m starshade for Roman Rendezvous mission
- Detailed design of all exposed edges and surfaces, e.g. undercut walls, edge radii and tapers.
  - Used FRED ray trace program, typically  $> 100M$  rays
  - Lacks detail at petal bases and inner disk termination at hub.
  - Includes pop-up stiffening ribs.
- INTEGRATED MAGNITUDE  $\sim V=29.5$ .
- AVERAGE MAGNITUDE AT IWA = 32.5. *Most of the light is at  $r < \text{IWA}$ .*
- Key Tolerances: petal piston,  $\pm 0.6$  mm, petal twist  $\pm 0.086$  deg, petal tilt  $\pm 0.036$  deg (5 mm at tips).



See Martin, Ellis, Shaklan et al, SPIE 11823 (2021)

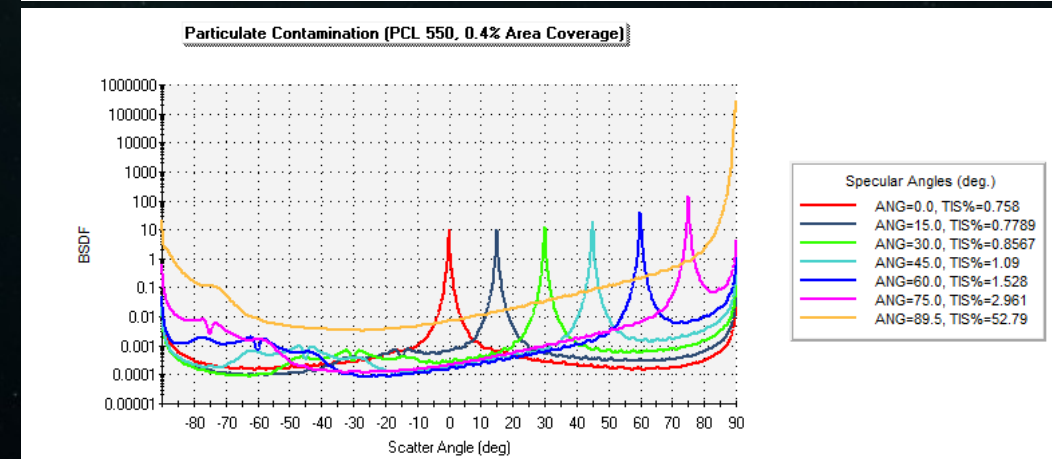
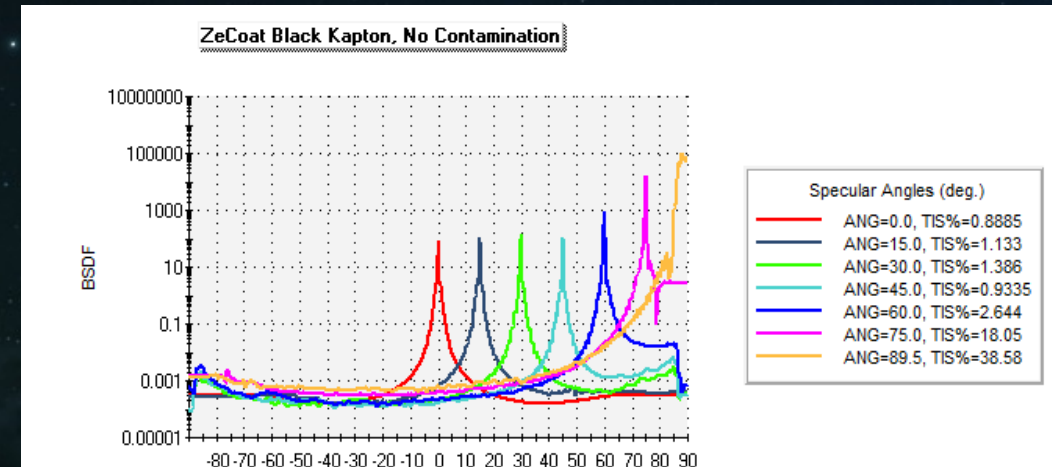
# STRAY LIGHT COATINGS AND CONTAMINATION

Our study assumes that most surfaces are coated with anti-reflection multi-layer or absorptive coatings. It assumes that all surfaces have particulate contamination (0.4% area coverage).

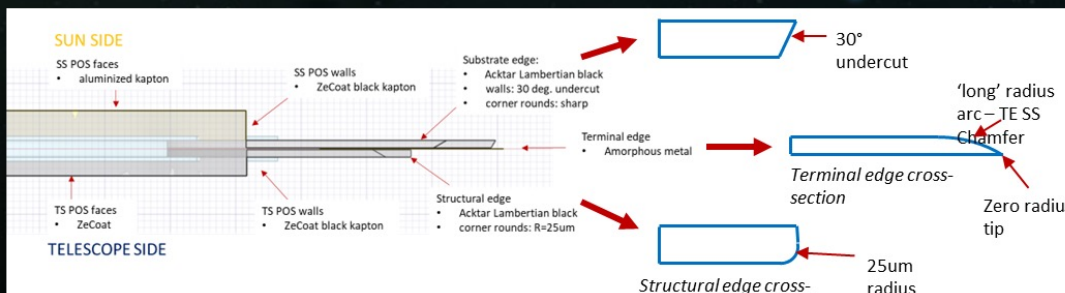
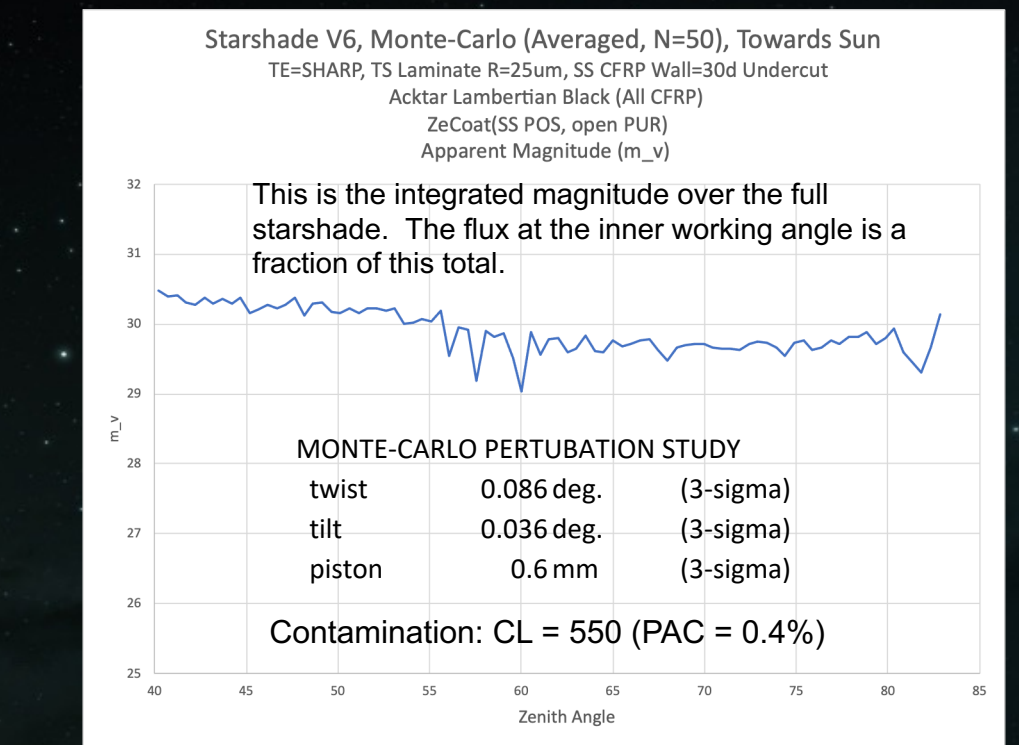
- Coating performance is measured or based on published values.
- The telescope-facing side is coated with a Zecoat black AR coating, as are the pop-up ribs.
- All CFRP is coated with Acktar Lambertian Black
- The contamination level is PCL 550, Percent Area Coverage = 0.4%.



*Photo of multilayer membrane 0.5 m wide coated by Zecoat under a Phase II SBIR. (Courtesy David Sheikh, Zecoat Corp.)*

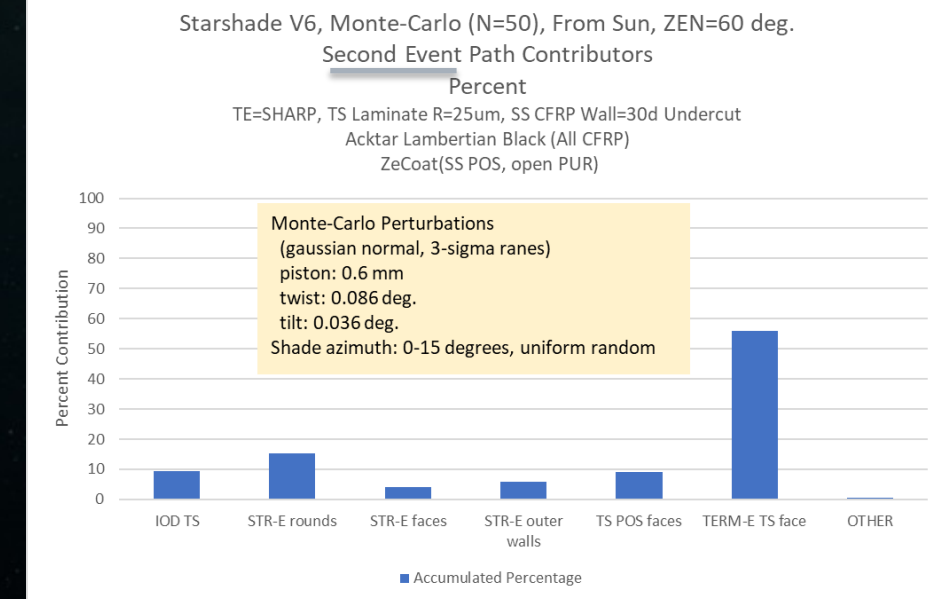
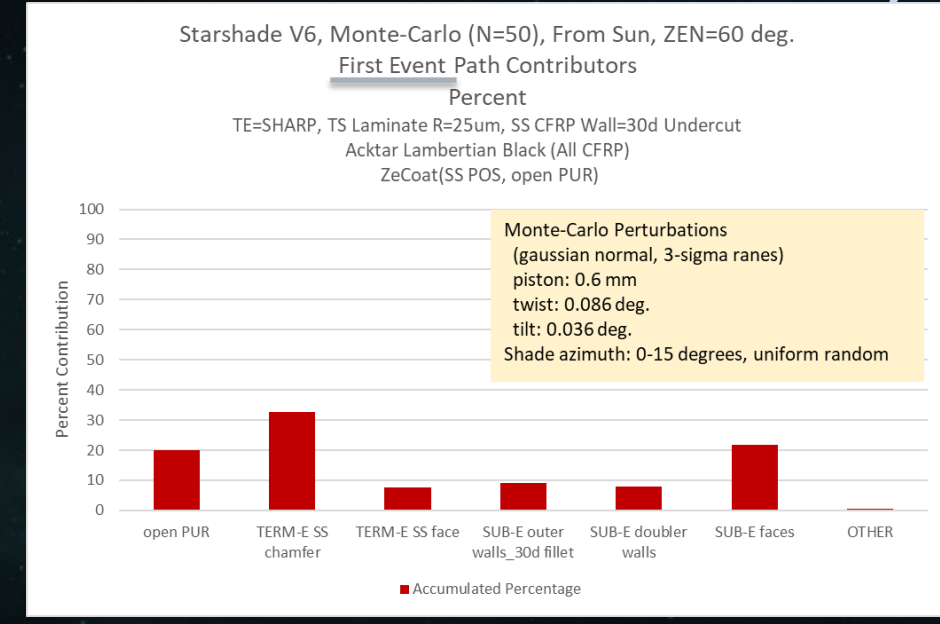


# STRAY LIGHT (OTHER THAN SINGLE EDGE SCATTER)



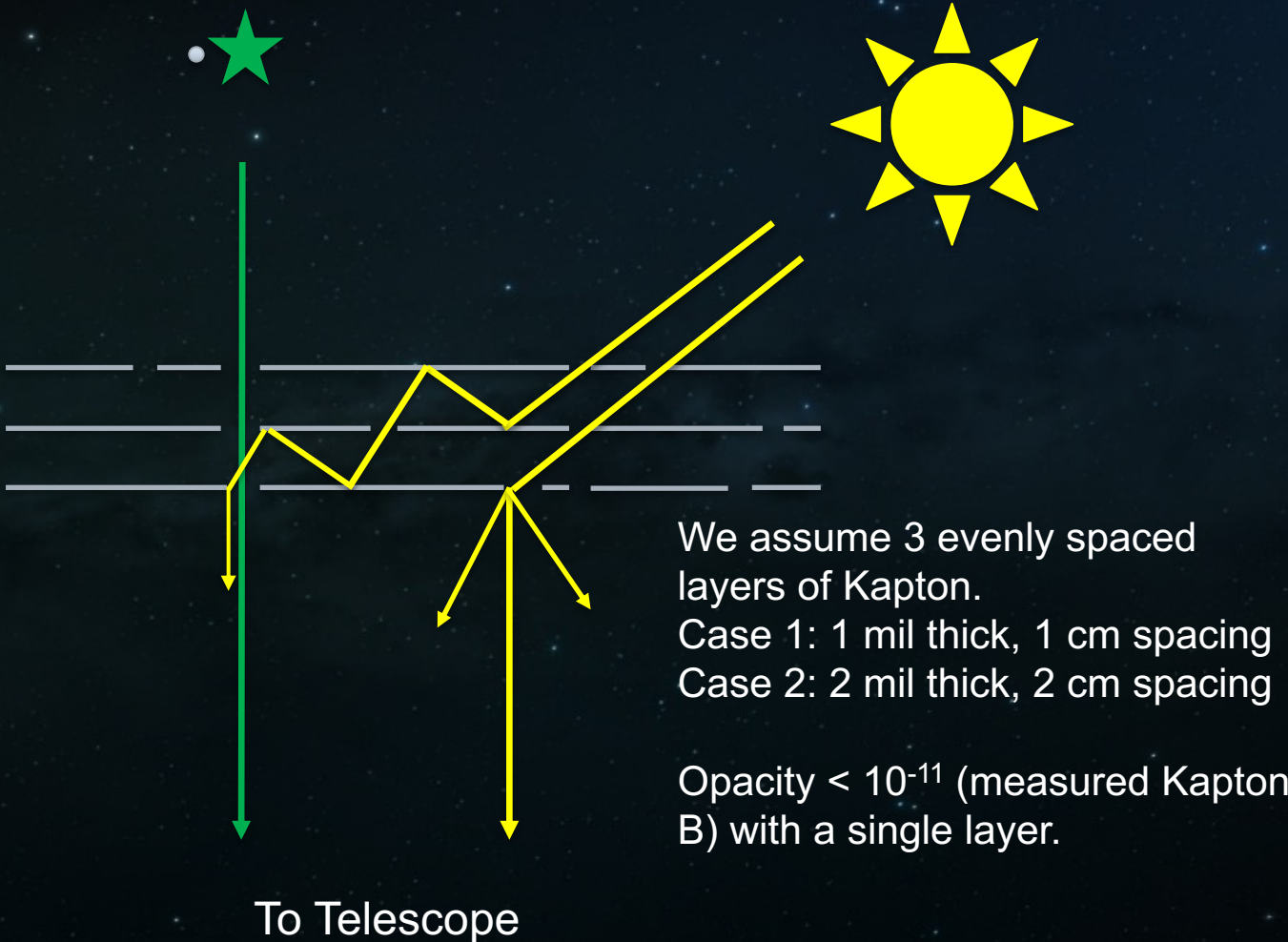
Terminal Edge components

- \* TS round = none (perfect point at edge)
- \* TS faces - flat section of terminal edge, telescope side
- \* SS chamfer - sloping face of terminal edge, sun side
- \* SS faces - flat section of terminal edge, sun side



# MICROMETEOROIDS: STARLIGHT AND SUNLIGHT LEAKAGE

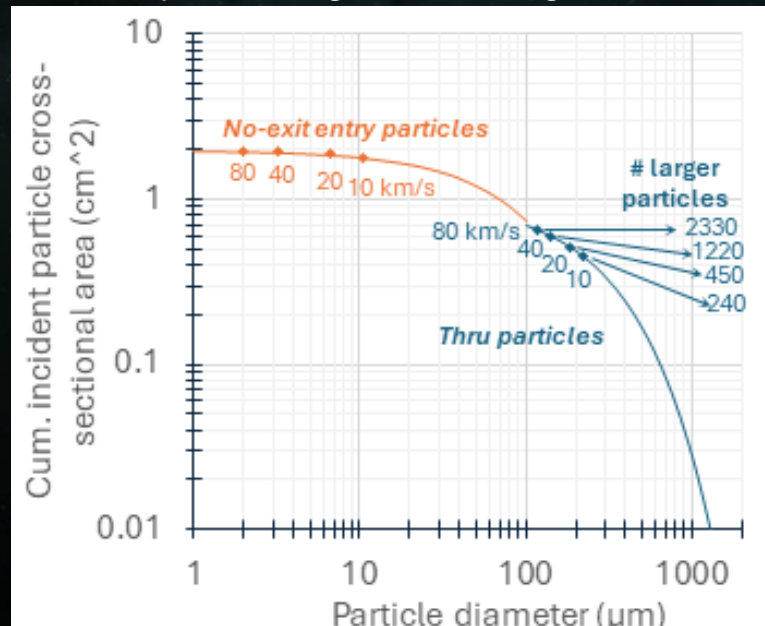
- Many randomly placed holes in all layers.
- Through holes aligned from star to telescope are rare.
- Through holes aligned to the direction of the Sun are rare.
- The brightest source of scatter is Sunlight going directly through the starshade then scattering at the edge of the bottom hole.
- The next brightest source of scatter is starlight going straight through the starshade.
- The third brightest source is sunlight scattering inside the starshade then scattering at bottom holes.
- Other paths are negligible.



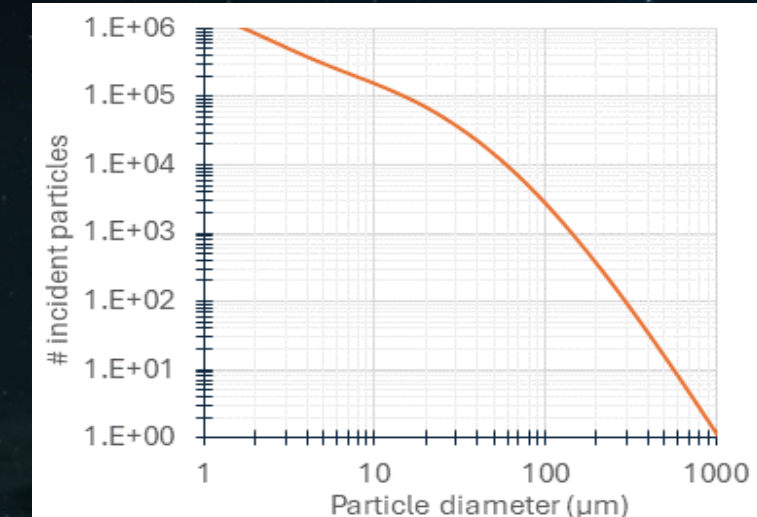
# MICROMETEOROIDS: STUDY ASSUMPTIONS

- Particles: silica, specific gravity = 2 (conservative)
- For hole analysis, specific gravity = 1 (aggregates)
- Use JWST Environments Specification (EV1-0074, 2009) for velocities.
- In-plane and out-of-plane impact velocities of 10, 20, 40, and 80 km/s, accounting for starshade velocity.
  - 80 km/s is 15% of particles but most of the hole area
- Exit/entry hole diameter ratio is only tested up to 15 km/s. This ratio is a free parameter in our study to allow growth for higher velocities.

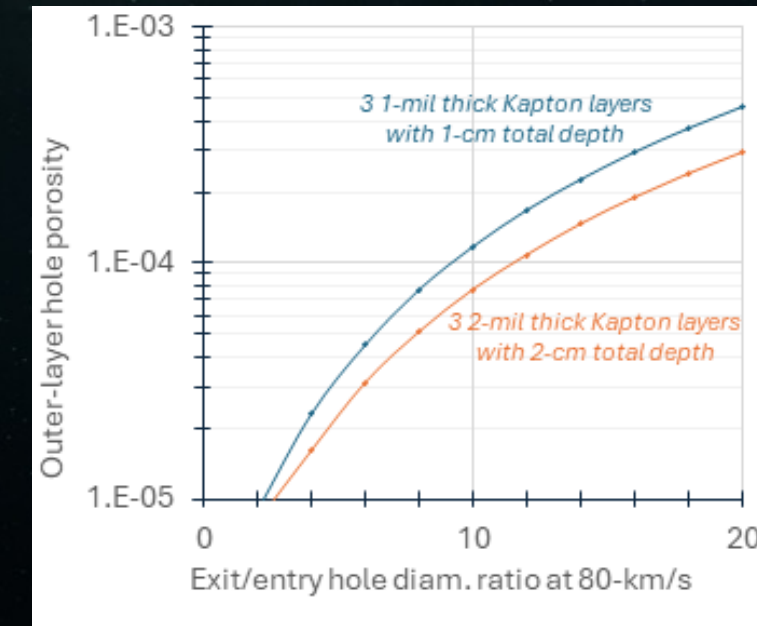
Minimum penetrating diam, through-hole counts



Number of incident particles (10 yrs) for 1/4 population

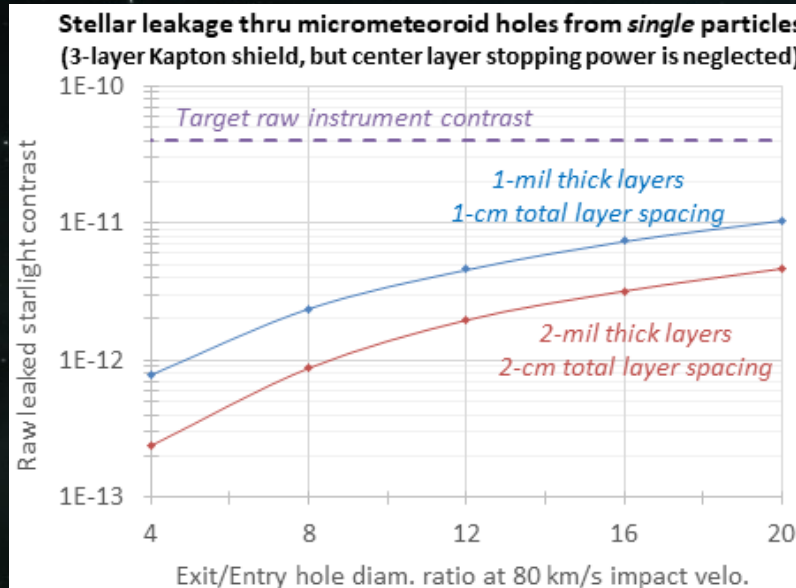


Hole porosity in outer layers vs. exit/entry hole ratio

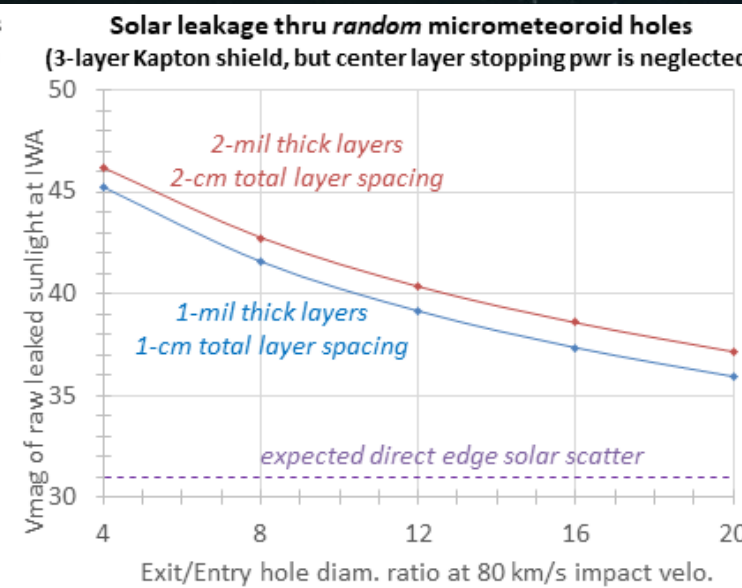


# MICROMETEOROIDS: MAGNITUDE OF SCATTER AFTER 10 YRS

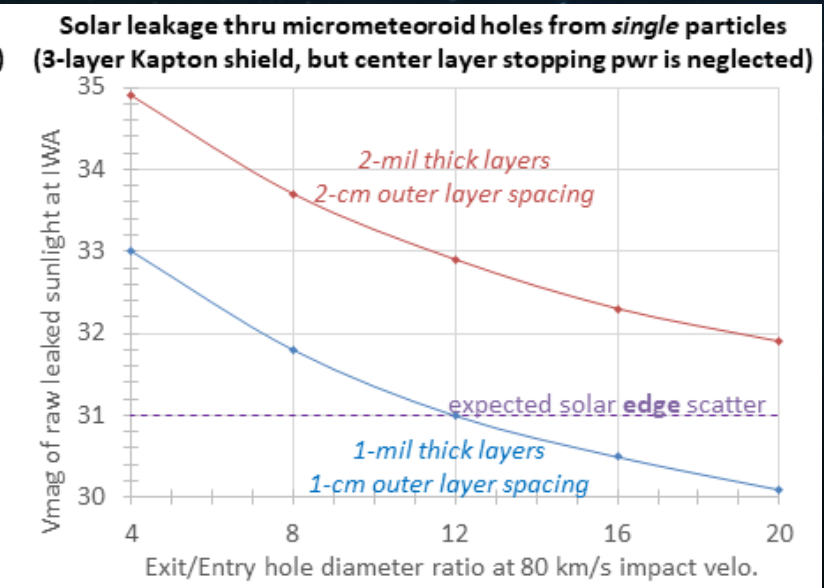
Straight Through Starlight



Sunlight, multiple bounces

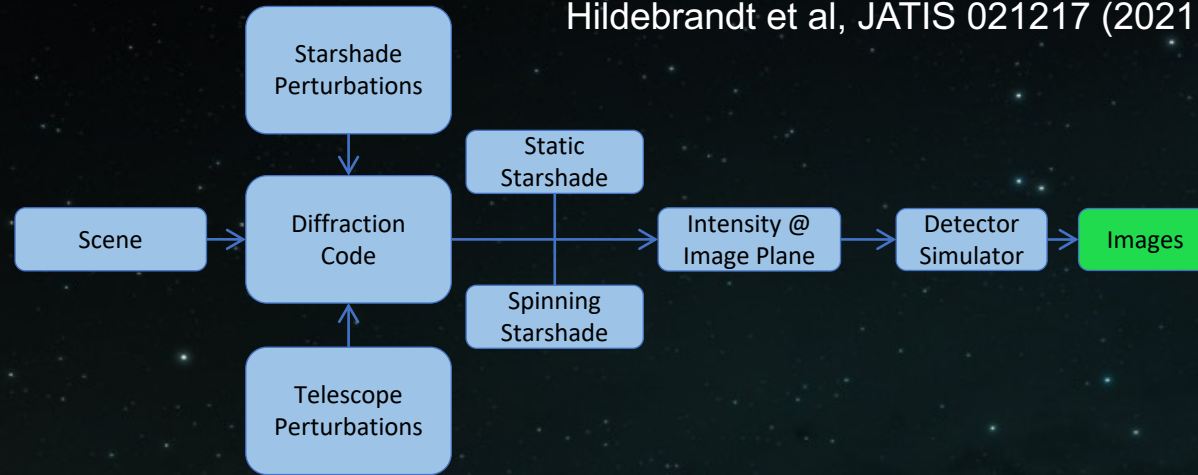


Sunlight, straight through + scatter

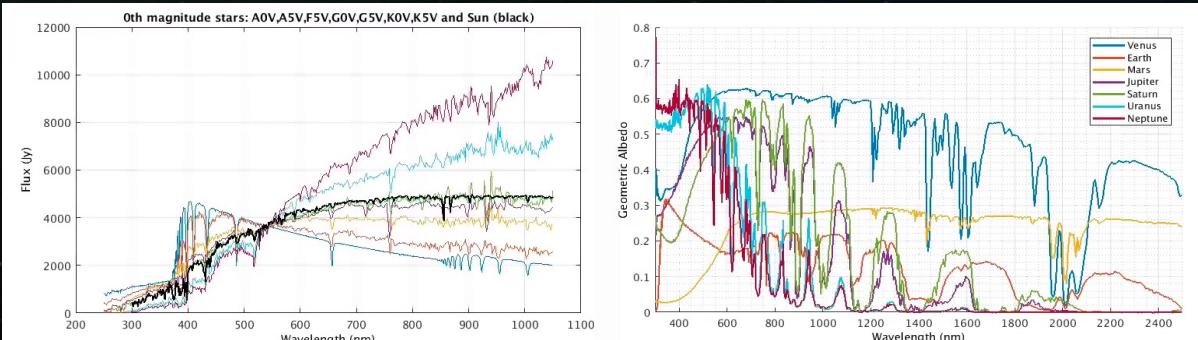


# SIMULATION TOOLKIT: SISTER

Hildebrandt et al, JATIS 021217 (2021)



- Any star in ExoCAT can be selected, or stars can be defined by the user through a few simple parameters.
- Stellar spectra are represented to the nearest 0.5 spectral type.
- Spectra are integrated over the user-selected imaging band.
- User can specify a planet in static position or a Keplerian orbit.
- User can specify planet characteristics ( $r$ , albedo) or choose a solar-system planet with a spectrum from Haystacks
- Choose from Lambertian or Rayleigh phase function, or specify the phase.

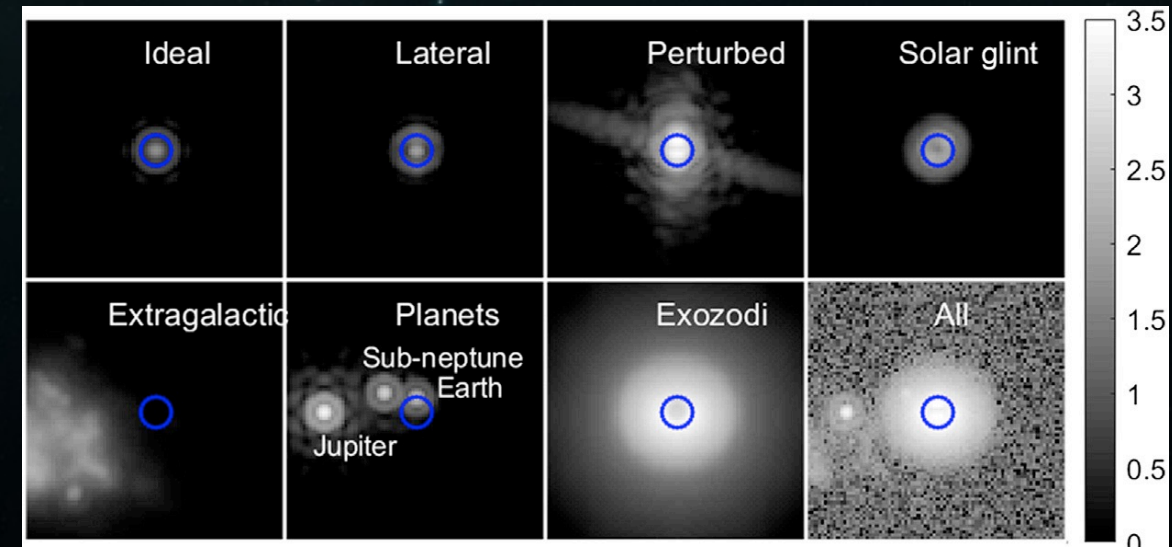


SISTER was developed by Sergi Hildebrandt, JPL/Caltech.  
Code/handbook available at [Sister.Caltech.edu](http://Sister.Caltech.edu)

1. **Telescope:** primary, secondary mirror, pupil, optical efficiency, pointing jitter.
2. **Detector model:** read noise, dark current, Filters, QE. For WFIRST.
3. **Starshade mode:** spinning, or non-spinning.
4. **Non-ideal Starshade:** shape deformations.
5. **Solar glint:** target Star-Starshade-Sun angle, and Sun angle about the orbital plane.
6. **Local Zodiacal light:** surface brightness model from STSCI, helio-centric coordinates.
7. **Star:** the user may define any star (its sub-spectral type will be approximated by either 0 or 5, e.g. G3 will be G5). Or one may choose among any of the 2,347 stars from ExoCat ([M. Turnbull, 2015](#)).
8. **Exo-dust emission:** any external model (for instance, from the Haystacks Project\*). SISTER has as a proxy a very simple model scaled, rotated and resized from one run of Zodipic.
9. **Planets and Keplerian orbits:** direct location, or 2-body motion with independent Keplerian parameters. No stability assessment.
10. **Reflected light from planets:** phase angle, phase functions (Lambert, Rayleigh).
11. **Extragalactic background:** deep field prepared by the Haystacks Project\*.
12. **Proper motion and parallax:** given star coordinates and proper motion.

## Imaging Capability Example

Intensities are displayed in log scale



# IMAGING SIMULATION: INSTRUMENT, SOLAR, EXOZODI, PLANET

Stellar  
Diffraction  
from  
deformed  
starshade.

Solar glint  
from petal  
edges

Solar leakage  
through  
micrometeorite  
holes + solar  
glint from non  
co-planar petals.

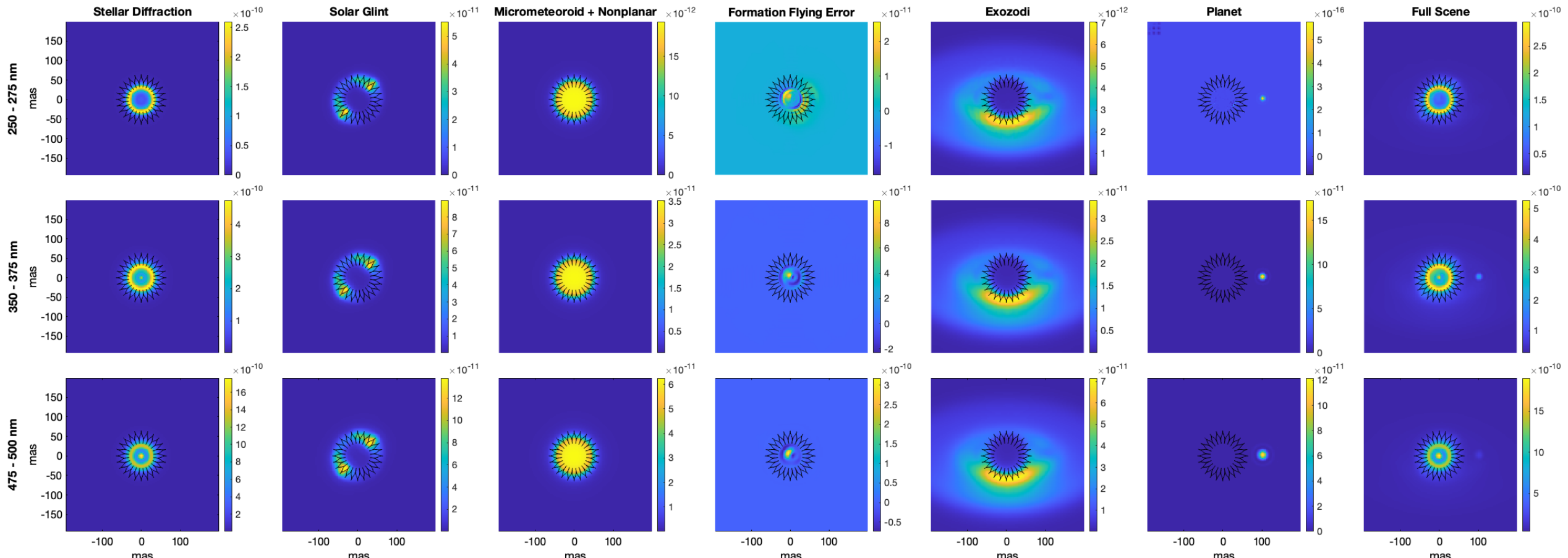
1-m formation  
flying offset.

Exozodi,  
density = 1,  
incl = 60 deg.

Exo-earth at 1  
AU, at  
quadrature

All  
components  
combined

Target star is a solar twin at 10 pc



# IMAGING SIMULATION: INSTRUMENT, SOLAR, ExOZODI, PLANET

# Stellar Diffraction from deformed starshade.

## Solar glint from petal edges

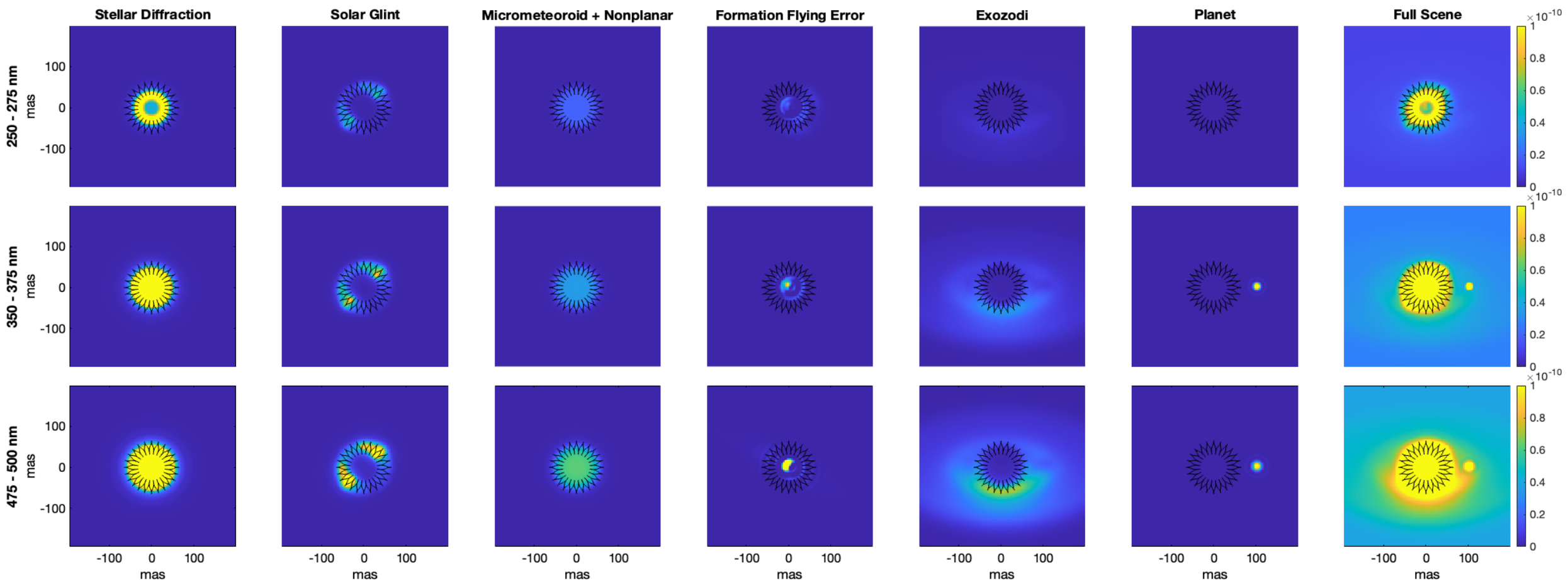
Solar leakage  
through  
micrometeorite  
holes + solar  
glint from non  
co-planar petals.

1-m formation flying offset.

Target star is a solar twin at 10 pc

## Exo-earth at 1 AU, at quadrature

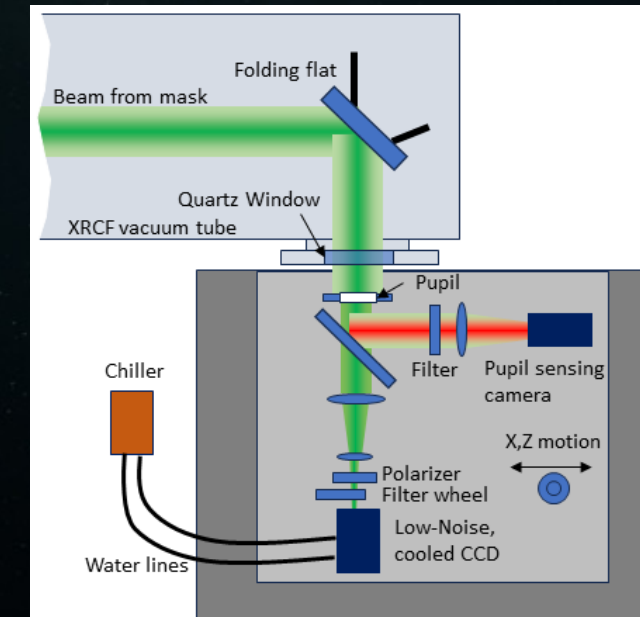
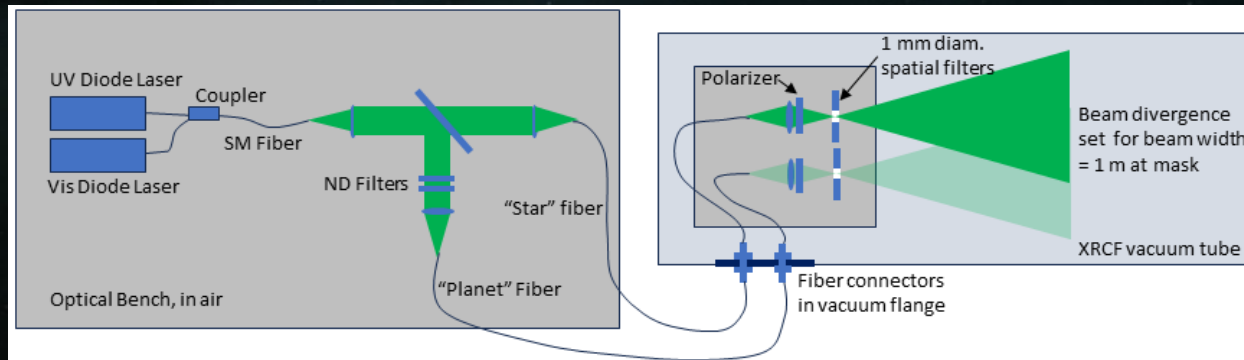
All  
components  
combined



# NEXT GENERATION OPTICAL TESTBED

The goal is to demonstrate end-to-end performance while observing an artificial planet in the UV in a laboratory experiment.

- Long baseline, 260 m, possibly at XRCF (MSFC).
  - Reduces polarization lobes 3x.
- Demonstrate observations at 250 nm (needs vacuum).
- Perform true broadband demonstration spanning 500-740 nm.
- Demonstrate active out-of-band formation control while observing in deep contrast.
- Demonstrate observations of a simulated planet.
- Spin the starshade about its axis, as is planned on-orbit.



# STARSHADE OPTICAL TECHNOLOGY SUMMARY

- **Optical Diffraction:**
  - Demonstrated  $< 1e-10$  contrast, broadband, model validation at flight Fresnel Number, showed contrast improving with angle
  - Measured sensitivity to shape errors. The measured Model Uncertainty Factor is included in starshade error budgets.
- **Formation Flying:**
  - Optical demo of sensing signal, model of alignment and telescope pointing, showed lateral sensing accuracy of 10 cm on an  $m_v = 8$  star (equivalent noise), hardware in the loop demo.
- **Solar glint:**
  - Measured edge sharpness, measured scatter of coated and uncoated edges, showed that edge glint will be  $\sim m_v = 31$  on HWO.
  - Measured scatter from particulate contaminants, developed link between edge particulate and surface particulates, developed edge contamination requirements.
  - Detailed modeling of surfaces and interfaces shows that glint from contamination will be  $\sim m_v = 32$  on HWO.
  - After 10 years on orbit, Micrometeoroid holes will scatter about as much sunlight as edge glint.
- **Next Generation Testbed:**
  - At 260 m long, it will reduce the polarization to below  $6e-11$  at the IWA and will include an artificial planet, a spinning starshade, and out-of-band formation control.

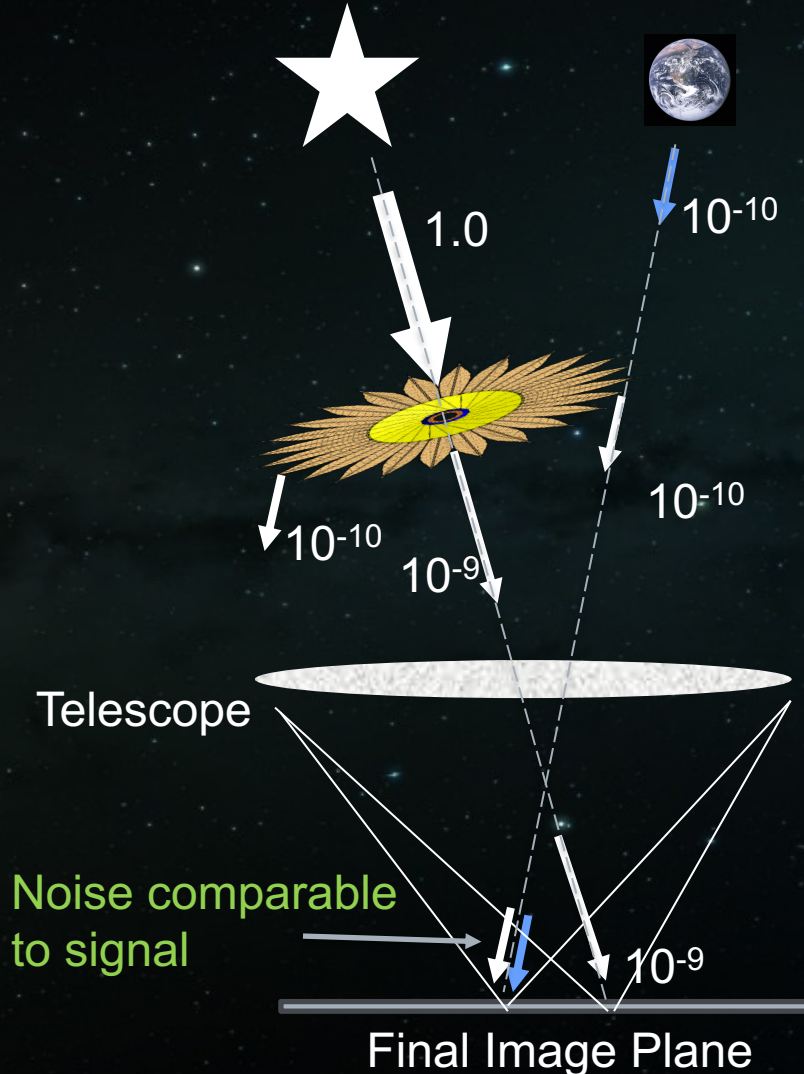
# STARSHADE OPTICAL TECHNOLOGY RELEVANCE TO HWO

- **Optical Diffraction:**
  - Demonstrated in 640-725 nm, compared to HWO need for 250 nm – 1000 nm
  - Single mask at laboratory scale will not work over the full band.
  - HWO is at larger Fresnel number and larger  $\lambda/D$  (better resolved by telescope), making it a much less challenging experiment optically
  - Longer scale to reduce polarization will increase the challenges (250 m vs 80, much greater environmental challenges unless in vacuum).
- **Formation Flying:**
  - No important differences. Same out-of-band sensing approach, large signal. Likely easier for HWO due to telescope resolution.
- **Solar glint:**
  - Demonstrated performance, including coatings, in the visible.
  - UV coatings are not expected to be more challenging (we are only going to 250 nm. **HOWEVER**, full broad-band coatings covering 250-1000 nm will be more challenging and we will likely have to accept a performance degradation.
  - All else being equal, the larger  $D/S^2$  (diameter / separation squared) makes HWO about 3.5 x easier than S5 baseline.
  - This is true for contamination and for scatter from micrometeoroid holes.

# BACKUP

# THE STARSHADE IS AN EFFICIENT FILTER

## Starshade



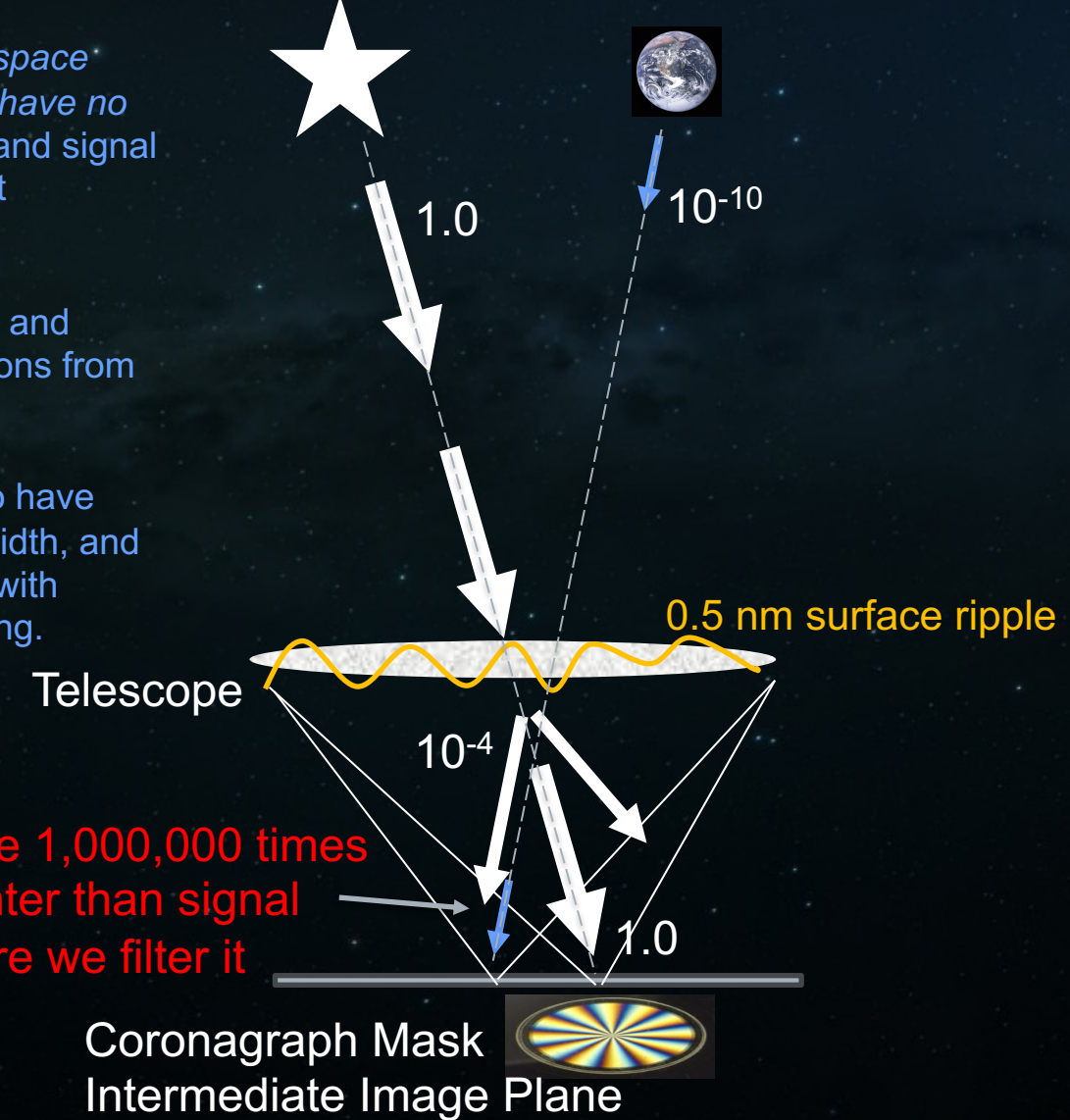
The planet photons are the signal.  
The stellar photons are the noise.

*The starshade is used in a space where the noise and signal have no overlap: the noise photons and signal photons come from different directions.*

The starshade is positioned and sized to block only the photons from the star.

This allows the starshade to have high efficiency, large bandwidth, and small working angle, along with readily achievable tolerancing.

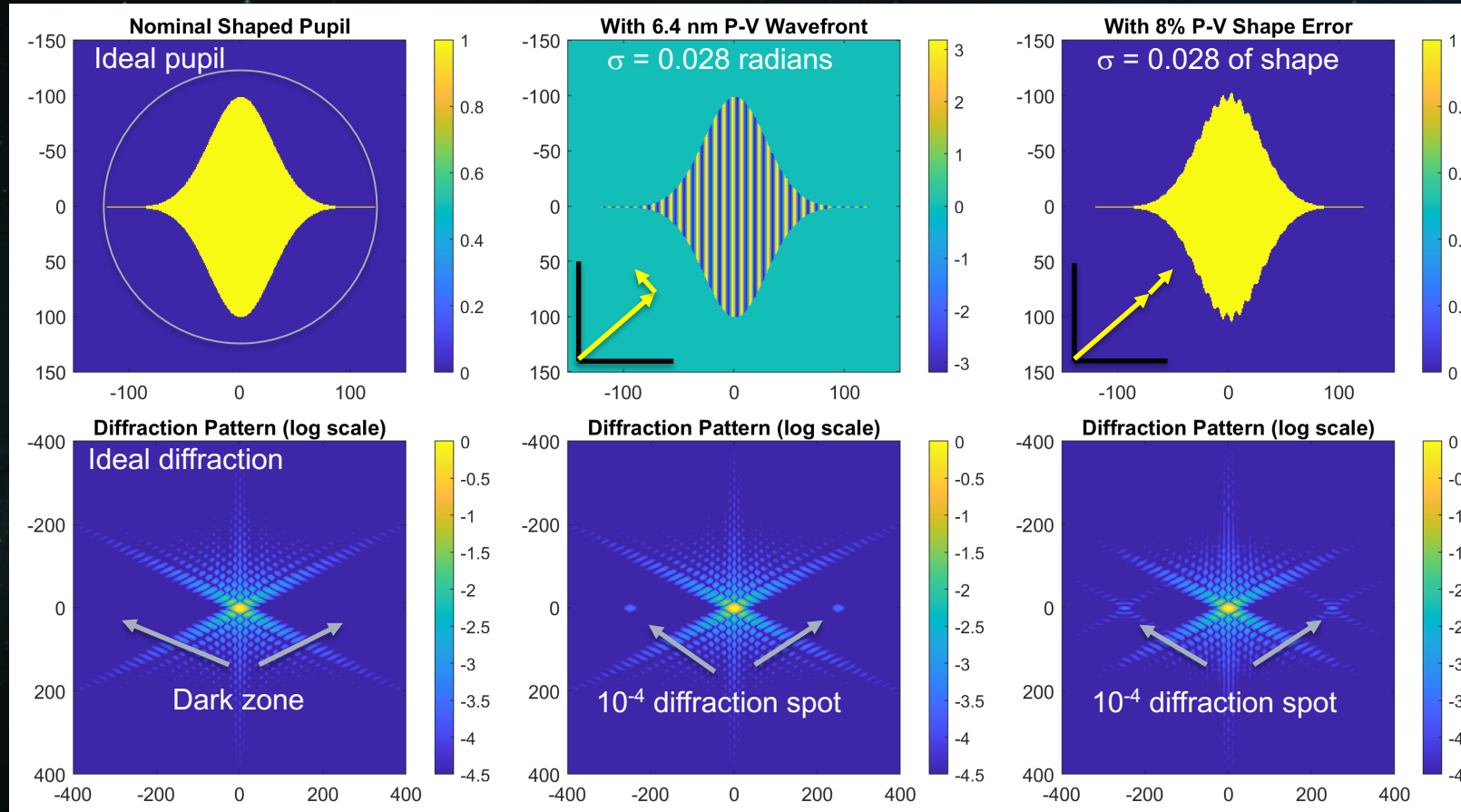
## Coronagraph



# SHAPE CONTROL IS EASIER THAN WAVEFRONT CONTROL

## AN EXAMPLE USING A SHAPED-PUPIL CORONAGRAPH

Shaped Pupil



Speckle Contrast:

$$C = \frac{\sigma^2}{2}$$

$\sigma$  is std. dev of phase in radians or, std. dev of fractional shape error.

Diffraction control using a shape is highly robust to errors.

As shown above, a few nm of wavefront error is equivalent to a few % shape error.

For  $10^{-10}$  contrast, 1 picometer of telescope wavefront is equivalent to 0.5 mm of starshade shape error.